6-2014

Object Detection using Dimensionality Reduction on Image Descriptors

Riti Sharma

Object Detection using Dimensionality Reduction on Image Descriptors

By

Riti Sharma

A Thesis Submitted in Partial Fulfillment of the Requirements for the Degree of
Master of Science in Computer Engineering

Supervised by

Dr. Andreas Savakis
Department of Computer Engineering
Kate Gleason College of Engineering
Rochester Institute of Technology
Rochester, NY
June, 2014

Approved By:

____Date:________________

Dr. Andreas Savakis
Primary Advisor – R.I.T. Dept. of Computer Engineering

____Date:________________

Dr. Raymond Ptucha
Secondary Advisor – R.I.T. Dept. of Computer Engineering

____Date:________________

Dr. Shanchieh Jay Yang
Secondary Advisor – R.I.T. Dept. of Computer Engineering

Dedicated to my parents Dr. Shakti Datt Sharma, Dr. Puja Sharma

and my sister Kriti Sharma

Acknowledgements

First and foremost, I would like to express my gratitude to my advisor and mentor, Dr. Andreas Savakis, for his invaluable guidance, patience, and immense knowledge. His confidence and faith in me, encouraged me. He supported me throughout my research and allowed me to grow and I thank him for his invaluable advice. Without his supervision and expertise; this work would not have been possible. I am extremely grateful to Dr. Ray Ptucha for his advice, and support on both academic and personal level. I thank him for his confidence in me and for serving as my committee. I would also like to thank Dr. Shanchieh Jay Yang, for serving as my thesis committee. His guidance motivated me.

I am extremely grateful to Richard Tolleson for his help throughout my work and I would also like to thank my fellow lab mates in Real Time Vision and Image Processing Lab- Bret Minnehan, Faiz Quraishi, Henry Spang, Ethan Peters, and Jack Stokes for their support, endless discussions and all the fun that we had in the lab.

I have no words to express my gratitude to my family for their endless love, concern, support and strength all these years and my friends for their continued encouragement.

Abstract

The aim of object detection is to recognize objects in a visual scene. Performing reliable object detection is becoming increasingly important in the fields of computer vision and robotics. Various applications of object detection include video surveillance, traffic monitoring, digital libraries, navigation, human computer interaction, etc. The challenges involved with detecting real world objects include the multitude of colors, textures, sizes, and cluttered or complex backgrounds making objects difficult to detect.

This thesis contributes to the exploration of various dimensionality reduction techniques on descriptors for establishing an object detection system that achieves the best trade-offs between performance and speed. Histogram of Oriented Gradients (HOG) and other histogram-based descriptors were used as an input to a Support Vector Machine (SVM) classifier to achieve good classification performance. Binary descriptors were considered as a computationally efficient alternative to HOG. It was determined that single local binary descriptors in combination with Support Vector Machine (SVM) classifier don’t work as well as histograms of features for object detection. Thus, histogram of binary descriptors features were explored as a viable alternative and the results were found to be comparable to those of the popular Histogram of Oriented Gradients descriptor.

Histogram-based descriptors can be high dimensional and working with large amounts of data can be computationally expensive and slow. Thus, various dimensionality reduction techniques were considered, such as principal component analysis (PCA), which is the most widely used technique, random projections, which is data independent and fast to compute, unsupervised locality preserving projections (LPP), and supervised locality preserving projections (SLPP), which incorporate non-linear reduction techniques.

The classification system was tested on eye detection as well as different object classes. The eye database was created using BioID and FERET databases. Additionally, the CalTech-101 data set, which has 101 object categories, was used to evaluate the system. The results showed that the reduced-dimensionality descriptors based on SLPP gave improved classification performance with fewer computations.

Table of Contents

List of Figures

List of Tables

Chapter 1

Introduction

Vision is one of the most important senses used by humans. The human brain can recognize many objects effortlessly, even though the objects may appear differently depending upon the viewpoint, illumination, etc. Objects can even be detected if there are occlusions caused by other objects. We can group instances of objects, such as fruits, pedestrians, cars, etc. into a single object class and can still differentiate between specific objects like “my own car” and “some other car”. This is far from straight forward for a computer. There are so many efforts being made to build machines that can see as humans do, yet we cannot escape that such capability is still far ahead of us.

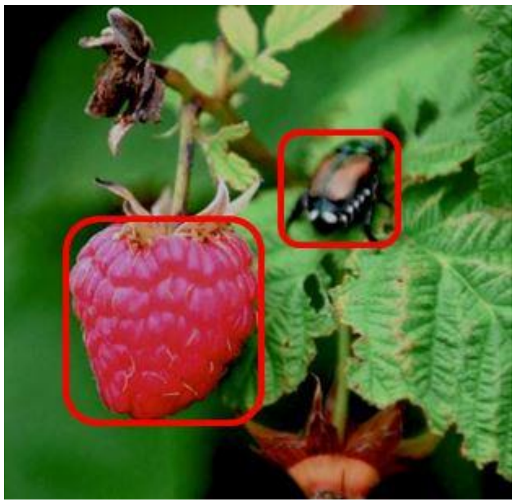

Figure 1.1: Example of Object Detection.

Object detection can be divided into two categories. The first category involves detecting an object class, for example detecting bananas from a fruit basket, and the second is detecting or recognizing a specific object, for example detecting a specific book from a book shelf.

1.1 Why is Object Detection Important?

Object detection is of great importance in the field of computer vision and robotics. It helps robots understand and interpret the world around them. Various applications include video surveillance, biometrics, traffic monitoring, digital libraries, navigation, interacting with human-computer interaction, etc.

We encounter applications using object detection in our daily lives, for example automatic driving and driver assistance systems in high end cars, human-robot interaction, immersive interactive entertainments, smart homes, assistance for senior citizens that live alone, and people finding for surveillance, security and military applications.

There are various challenges involved regarding detection of real world objects such as vehicles, animals, birds, people, etc. Real world objects have a lot of variation in terms of color, texture, shape and other properties. Also, objects can even have a wide variability in their appearance characteristics, due to lighting, size, pose, etc. The backgrounds against which the objects lie are often complex and cluttered as shown in Figure 1.5. For example, it might be easier for a robot to find or detect a book with nothing else present on a table, and quite difficult to detect the same book on a table that is cluttered by other objects. Images from Caltech-101 [53] database of objects at different distances and different viewpoints are shown in Figure 1.2 and 1.3 respectively. Figure 1.4 shows intra class variation.

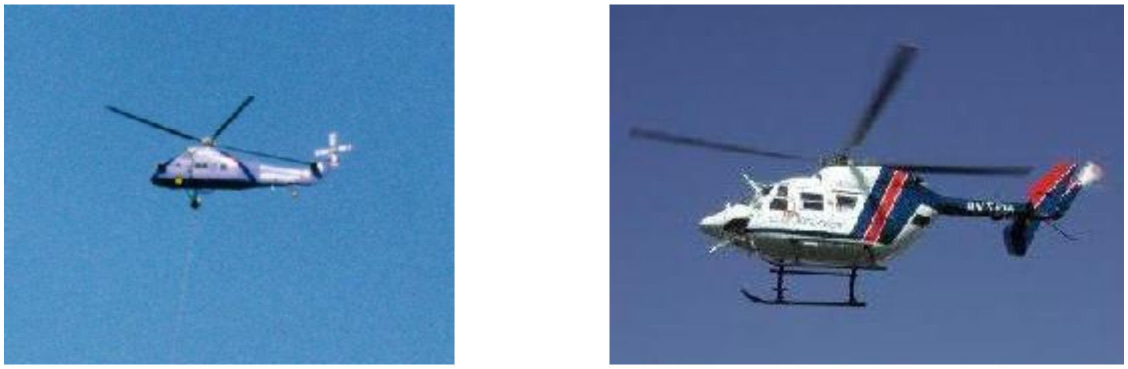

Figure 1.2: Images from CalTech-101 showing Objects at different Distances.

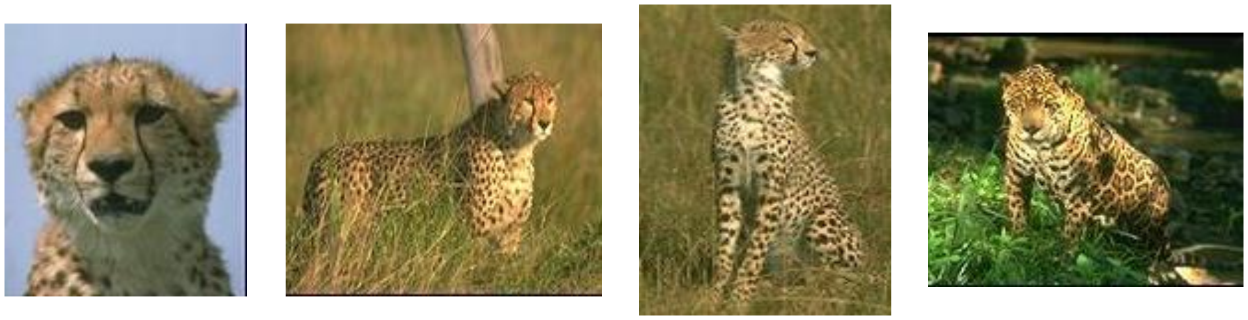

Figure 1.3: Images from CalTech-101 showing Objects with different Viewpoints.

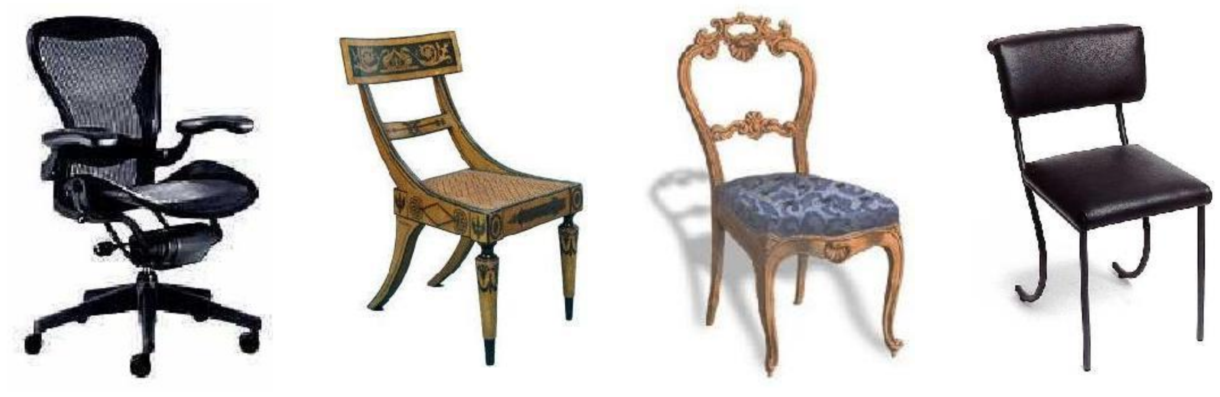

Figure 1.4: Images from CalTech-101 showing Intra Class Variation.

Figure 1.5: Image from CalTech-101 showing Object with Cluttered Background.

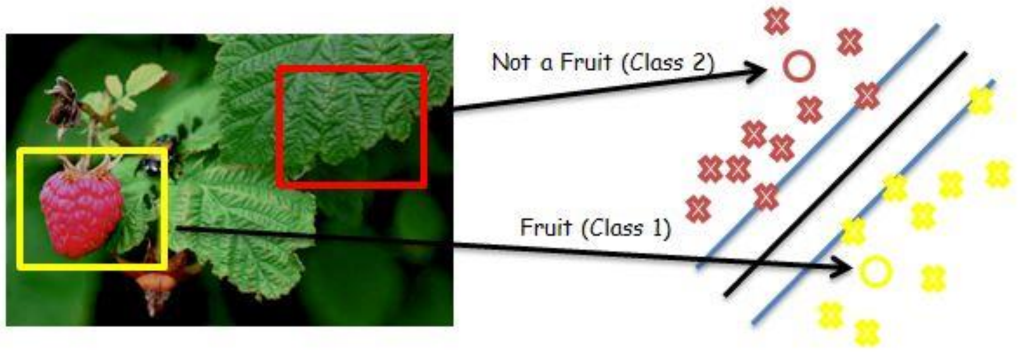

Figure 1.6: Sliding Window Example.

1.2 Methodology

In this thesis, sliding window based detectors are used. The entire image is scanned to extract patches, and these patches are classified into object or non-object category. The sliding window detection approach is shown in Figure 1.6.

This process can be broadly separated into the three stages of feature extraction, dimensionality reduction and classification. Figure 1.7 shows the process of detecting object from a given image.

In the feature extraction stage, the window of a fixed size is moved over an image, and for each location a feature descriptor is extracted. In this thesis, a histogram of binary descriptors is considered for object detection - in particular, the histogram of LBP and histogram of FREAK, are compared with the Histogram of Oriented Gradient descriptor.

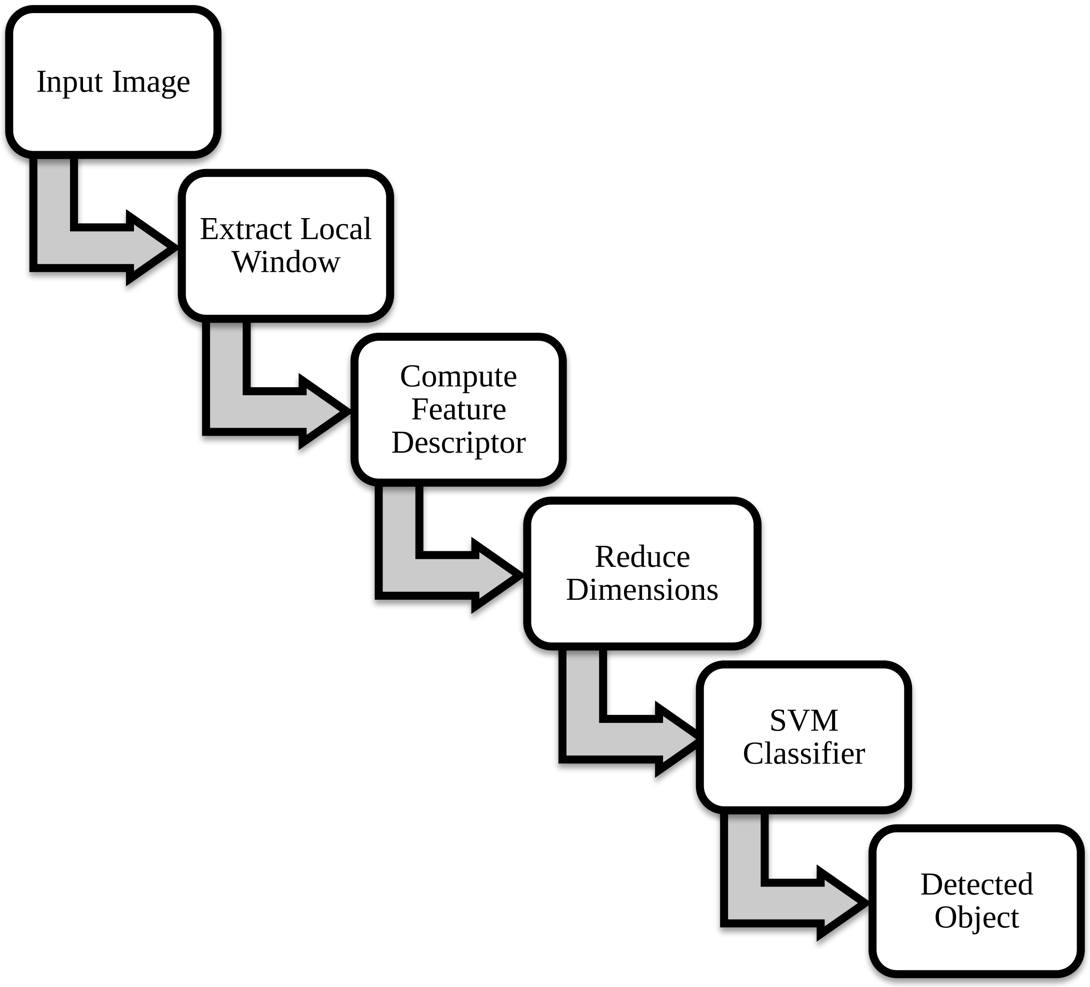

Figure 1.7: Sliding Window Detection Process.

The objective of dimensionality reduction is to project the data on a lower dimensional space while retaining the important properties of the data for the problem under consideration. Working with high dimensional data can be computationally intensive and slow. In cases where the feature space is extremely large, the effect known as the Curse of Dimensionality may result in lower performance compared to that of a lower dimensional feature space.

Dimensionality reduction offers computational benefits obtained by processing a smaller amount of data. A secondary benefit of dimensionality reduction is that some noise and redundancies in the features are eliminated after reducing the feature space. As a result, the data can be represented in a more compact and effective way, which can improve classifier performance. Techniques such as Principal Component Analysis (PCA), Linear Discriminant Analysis, and Manifold Learning have been used for subspace learning and dimensionality reduction [11, 12].

1.3 Thesis Contributions

This work proposes a holistic approach towards detecting object from images. The approach integrates different image feature descriptors with various dimensionality reduction techniques. The following summarize the contributions made in this thesis.

- Eye Detection
    - Efficient approach to detecting eyes using dimensionality-reduced Histogram of Oriented Gradients as feature descriptor
    - Evaluation of Principal Component Analysis, Random Projections, Locality Preserving Projections (LPP), and Supervised Locality Preserving Projections (SLPP) on image descriptors for eye detection.
    - The HOG-PCA descriptor, published by A. Savakis, R. Sharma, and M. Kumar, “Efficient Eye Detection using HOG-PCA Descriptor.” IS&T/SPIE Electronic Imaging Conference, Imaging and Multimedia Analytics in a Web and Mobile World, 2014 [44].

- Image descriptors
    - Proposed histogram-based FREAK descriptor as a feature descriptor for successful object detection.
    - Analysis of HOG, LBP, Histogram of LBP (H-LBP), FREAK, and Histogram of FREAK (H-FREAK) for the purpose of detecting objects.
- Dimensionality Reduction
    - Evaluation and analysis of various dimensionality reduction techniques, specifically PCA, Random Projections, LPP and SLPP for object detection.

1.4 Thesis Outline

Following the introduction, Chapter 2 gives a background about different approaches to object detection and discusses various methodologies.

Chapter 3 gives an overview of the different feature descriptors used in this thesis. It begins with the basic descriptor on a raw image and then migrates to the more sophisticated descriptors, such as Histogram of Oriented Gradients (HOG), Local Binary Patterns (LBP), and Fast Retina Keypoint (FREAK) descriptors.

Chapter 4 covers fundamental concepts of dimensionality reduction. It begins with the need and advantages of dimensionality reduction and gives an overview of the different dimensionality reduction techniques used in the thesis such as PCA, Random Projections, and Manifold Learning using LPP.

Chapter 5 discusses the support vector machine classifier. It begins with the basic idea behind the SVM classifier. It discusses the statistical learning theory behind the support vector machines and goes over the mathematics involved. It also discusses the bootstrap technique and various classification approaches.

Chapter 6 presents the eye detection system developed in this work. It begins with the motivation and related work for eye detection. It then presents the detailed approach for eye detection.

Chapter 7 discusses the different datasets used in this work for evaluation of the system and the results of using different descriptors for object detection. It also discusses the effects of using different dimensionality reduction techniques with these descriptors.

The Conclusion chapter summarizes the work of this thesis, discusses the key findings and offers some directions for future work.

Chapter 2

Related Work

Object detection has received a lot of attention in the field of computer vision. Learning algorithms used for object detection vary from simple k-nearest neighbor [3] to random forests [7, 8] and neural networks [19, 54]. The most popular among these classification methods is Support Vector Machines (SVM) [34, 35, 46, 47] which was introduced in [43] by Boser, Guyon and Vapnik.

In parts-based object detection, the object is treated as collection of different parts. Different parts are extracted from the object and detection is done using appearance and geometric information between parts. A popular and successful approach is the deformable parts model (DPM) [49]. The DPM breaks up the appearance of an object class into sub-classes which correspond to a different structure or pose. A part-based approach for human detection was used in [49], where a person was divided into components such as arms, legs, head, etc., and then support vector machine classifier was used in human detection. A sparse parts-based object detection was used in [45] to detect cars.

Bags-of-words descriptor with SVM classification is another popular approach for object recognition and is taken from text analysis. It converts the image into bag-of-words using three basic steps: feature detection which detects distinctive and repeatable image features from the image, feature description which extracts a feature descriptor from an image patch, and feature quantization which is used to quantize the descriptor into a word defined in a given codebook.

[68] use bag-of-word model with SIFT features and SVM for object detection. Also, bag-of-words descriptor is used in [67] for action recognition.

The approaches using parts-based model and bag-of-words model are efficient but more complex and computationally expensive. Furthermore, it is hard for these models to cope with a limited set of training data, whereas object detection based on treating objects as a single unit is simple and involves fewer computations.

Feature descriptors are used in many real world applications such as object detection, object tracking, etc. The emphasis is to learn features that are invariant to scale, viewpoint, illumination, etc., and thus are efficient. One popular feature is Scale Invariant Feature Transform, SIFT. In [36], an object recognition system was developed based on SIFT descriptors. Many variants to SIFT descriptor have also been proposed, such as Speeded Up Robust Features (SURT) [37] which was developed as a computationally efficient alternative. Dimensionality reduction in the form of Principal Component Analysis (PCA) was utilized to obtain PCA-SIFT [37], a descriptor with fewer components that offers good performance.

Another popular feature descriptor is the Histogram of Oriented Gradients (HOG). It was initially proposed for pedestrian detection by Dalal and Triggs [5]. Since then it has been adopted in the context of various classification problems [40, 41]. Dalal & Triggs [5] used histogram of oriented gradients with support vector machines classifier in a sliding window framework for pedestrian detection. A multi-scale part based object detection system using Latent SVM and HOG was built in [49] and is considered the state-of-the-art in object detection. Recently there is work done with structured learning to improve detection performance. In [16] Uricar and Franc proposed the use of structured SVMs for facial landmark detection and [9] employs structured learning for 2D pose estimation to improve pedestrian detection technique. The authors in [1] propose an approach in which separate SVM classifiers are trained for each object instance, and each of these classifiers consists of a single positive example and many negative examples.

In contrast to SIFT, HOG is a dense descriptor and this encouraged the use of dense binary descriptors for object detection. Local Binary Pattern has been popular in many classification problems, such as texture classification [32], face recognition [31], etc. Recently, HOG-LBP based descriptor was also used for object localization [30, 29].

Other binary descriptors include BRIEF [28] which uses binary tests between pixels in a patch to build a descriptor that is robust to lighting, blur and perspective distortion; BRISK [10] produces keypoints that are scale invariant. Recently FREAK [39] was introduced as a robust binary descriptor and it is invariant to viewpoints, illumination or rotation variations.

However, there is a lack of approaches that consider binary descriptors for object detection. Most importantly, which binary features are stable and flexible for object detection or recognition still remains an unanswered question. Since binary descriptors are computationally efficient, this thesis considers histogram of binary descriptors as an alternative to HOG for object detection in addition to the exploration of dimensionality reduction techniques.

Chapter 3

Image Descriptors

To be able to successfully detect an object or classify objects into different categories, we must be able to describe the properties of an object in a unique manner. In order to accomplish this, the descriptors must have certain properties that make them unique, reproducible, invariant and efficient. Firstly, similar objects should have similar descriptors. Thus, objects should be classified to a particular category only if they have similar descriptors. Secondly, the descriptors should be invariant to scale, rotation, and illumination. In addition, they should be invariant to perspective changes as the object could be observed from a different viewpoint. The descriptors should be compact and should only contain the information that makes the object unique. Figure 3.1 shows an example image and its variation due to rotation, illumination and scale.

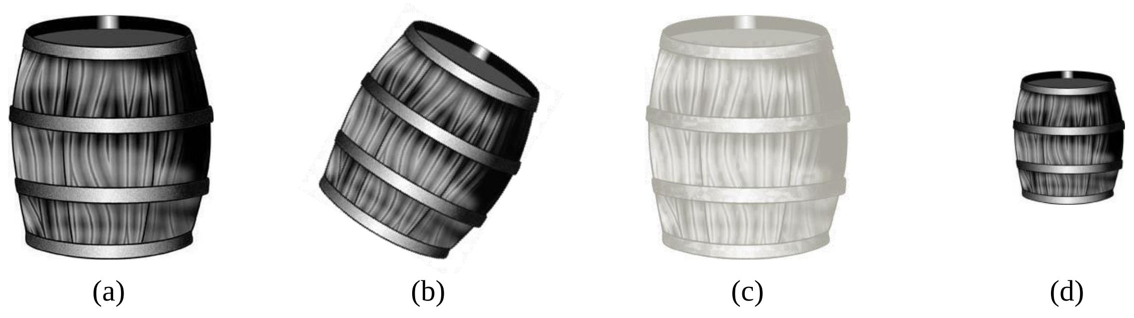

Figure 3.1: Images from CalTech-101, (a) Original Image, its variations due to (b) Rotation, (c) Illumination, and (d) Scale.

3.1 Low Level Image Descriptors

The low level image descriptors are computed directly from the image pixels. For example a color histogram is a low level feature extraction method. Low level image descriptors are defined to capture a certain visual property of an image either globally for the entire image or locally for a group of pixels in a particular region. These local features are based on color, texture, shape, motion etc. [5]. These descriptors have been used extensively for image retrieval. For example [59] uses color, texture and shape features combined for content based image retrieval. [25] uses texture based features to classify maritime pine forests images. These descriptors are not well suited for object detection and thus there is a need for better image descriptors.

3.2 Histogram of Oriented Gradients

The success and broad application of the SIFT keypoint descriptors [36] has motivated the development of various local descriptors based on edge orientations. The Scale Invariant Feature Descriptor was introduced by David Lowe and is designed to be invariant to translation, scaling, rotation and to some extent, illumination. Keypoint detection is the first stage of SIFT feature extraction which identifies key locations as maxima and minima of the result of difference of Gaussians (DOG) function, applied in scale space to a series of smoothed and resampled images. Low contrast candidate points and edge response points along an edge are discarded. Dominant orientations are assigned to localized keypoints and a feature vector is formed by specifying the orientation relative to the keypoint, essentially making the vector rotation invariant. The major drawback of SIFT feature descriptor is that it is computationally expensive. SIFT was originally developed for image stitching and used for panorama construction [55], while object detection was considered as a secondary application. SIFT is designed to be a sparse descriptor that identifies keypoints of interest, which is a different approach than that of dense descriptors such as HOG, which was developed with object detection in mind.

The Histogram of Oriented Gradients is a popular descriptor that was initially proposed for pedestrian detection by Dalal and Triggs [5]. Since then it has been adopted for various classification problems. In [26] HOG features were used for detection of human cells, and in [27] for vehicle detection. In [2] HOG features were proposed for face recognition. The process of generating HOG Descriptor for an image is shown in Figure 3.2.

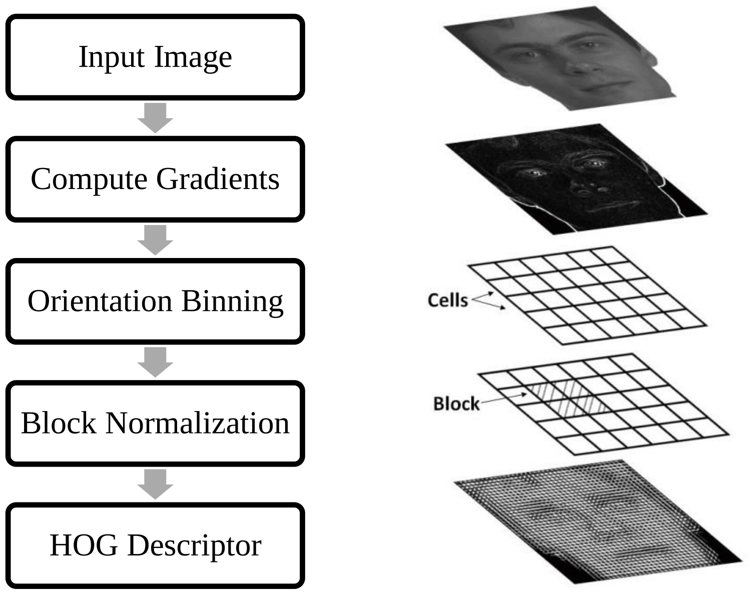

Figure 3.2: Process of formation of Histogram of Oriented Gradients feature descriptor.

To obtain the HOG features, the gradient of the image is computed by applying an edge mask. A simple 1-D mask of the form [-1, 0, 1] works well. More complex masks, such as Sobel operator and others were tested in [5], but the simple, centered, 1-D derivative mask works the best. The resulting gradient image is divided into smaller non overlapping spatial regions called cells. These cells can be rectangular, which results in the R-HOG descriptor, or circular, which results in the C-HOG descriptor, as shown in Figure 3.3. Each pixel in the cell casts a vote that is weighted by its gradient magnitude, and contributes to an orientation aligned with the closest bin in the range 0-180 (unsigned) or 0-360 (signed). The orientations of the bins are evenly spaced and generate an orientation histogram. This step is known as Orientation Binning. After Orientation Binning, the cell histograms are normalized, for better invariance to illumination and contrast. The cells are grouped together in 2x2 overlapping blocks and each of these blocks is normalized individually. The overlapping of blocks ensures that there is no loss of local variations and there is a consistency across the whole image.

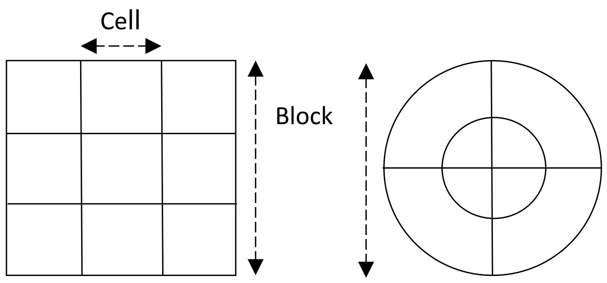

Figure 3.3: Rectangular and Circular Cells, used in Histogram of Oriented Gradients.

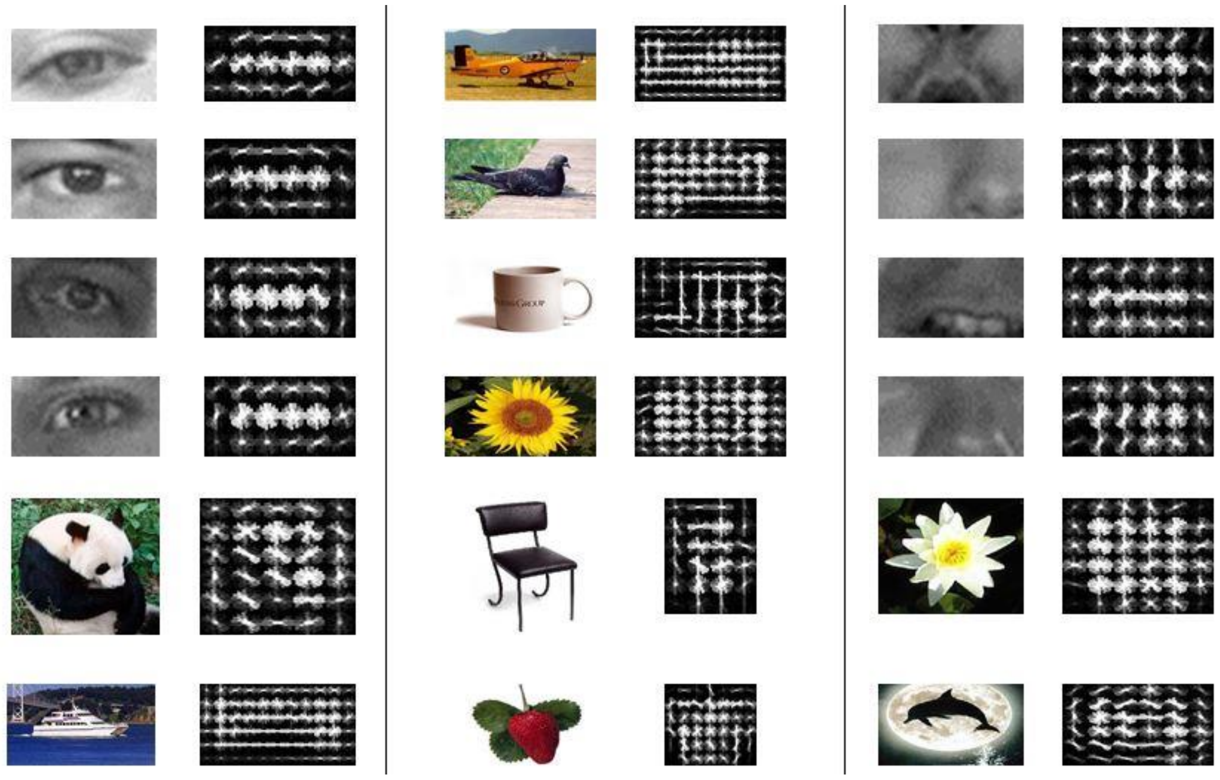

Figure 3.4: Sample Images and their HOG Descriptor.

Figure 3.4 shows examples of images and their HOG descriptor. The HOG descriptor has proven effective for classification purposes and has been applied on a variety of problems. Its main disadvantage is the associated computational load. When considering invariance, HOG features are somewhat invariant to illumination.

3.3 Binary Descriptors

In Histogram of Oriented Gradients, the gradient of each pixel in a patch needs to be computed. This makes it computationally expensive and thus, is not fast enough for some of the applications. Local binary descriptors, where most of the information can be encoded into a binary string using comparison operations, are more computationally efficient. In addition, matching between binary descriptions can be done by the Hamming distance, i.e. just counting the number of bits by which they differ. This is the same as using the sum of the XOR operation between two binary strings.

Binary descriptors are composed of three parts: sampling pattern, the pattern by which points need to be sampled in a given region; sampling pairs, these are the pairs which are compared in order to build the descriptor; and orientation compensation, the method used to make the descriptor rotation invariant or algorithm to find the orientation of a given keypoint. In order to construct a binary string, we compare the intensity values at the two given points. If the intensity value of the first point is greater than the second, we add a 1 to the binary string; else we add a 0 to the binary string. Examples of binary descriptors include LBP, BRISK, FREAK, etc.

3.4 Local Binary Patterns

The Local Binary Pattern (LBP) descriptor is the simplest binary descriptor and is a popular feature to describe the texture of an image. It converts each pixel into a binary number by thresholding the neighborhood of each pixel. In this descriptor the given image is divided into integer blocks. For each of these blocks, the center pixel is considered as the threshold value and its other neighboring pixels are assigned 0 or 1 depending upon the intensity value of the center pixel. This results in a p-bit binary number, where p is the number of neighboring pixels. Figure

3.5 shows an example to generate LBP descriptor. It is invariant to any monotonic gray level change and is simple to compute.

$$\begin{array}{|c|c|c|}\hline 8 & 0 & 9 \\ \hline 5 & 6 & 6 \\ \hline 1 & 2 & 3 \\ \hline \end{array} \xrightarrow{Threshold} \begin{array}{|c|c|c|}\hline 1 & 0 & 1 \\ \hline 0 & & 1 \\ \hline 1 & 0 & 0 \\ \hline \end{array} * \begin{array}{|c|c|c|}\hline 1 & 2 & 4 \\ \hline 8 & & 16 \\ \hline 32 & 64 & 128 \\ \hline \end{array} = \begin{array}{|c|c|c|}\hline 1 & 0 & 4 \\ \hline 0 & & 16 \\ \hline 32 & 0 & 0 \\ \hline \end{array}$$

$$LBP \;=>\; 1 + 4 + 16 + 32 = 53$$

Figure 3.5: Example to find LBP Descriptor for a given Image.

The derivation of Local Binary Pattern descriptor as described in [42] is as follows:

Let $I(x, y)$ be an image and let g_c be the gray level of an arbitrary pixel (x, y). Let g_p be the gray value of a sampling point in an evenly spaced circular neighborhood of P sampling points and radius Raround the point (x, y).

$$g_p = I(x_p, y_p), \quad p = 0, \ldots, P - 1 \tag{3.1}$$

$$x_p = x + R\cos(2\pi p/P) \tag{3.2}$$

$$y_p = y - R\sin(2\pi p/P) \tag{3.3}$$

Assuming that the local texture of the image $I(x, y)$ is characterized by the joint distribution of gray values of $P + 1$ $(P > 0)$ pixels:

$$T = t(g_c, g_0, g_1, \ldots, g_{p-1}) \tag{3.4}$$

Without loss of information, the center pixel value can be subtracted from the neighborhood:

$$T = t(g_c, g_0 - g_c, g_1 - g_c, \ldots, g_{p-1} - g_c) \tag{3.5}$$

Now, the joint distribution is approximated by assuming the center pixel to be statistically independent of the differences, which allows for factorization of the distribution

$$T \approx t(g_c) * t\big(g_0 - g_c, g_1 - g_c, \dots, g_{p-1} - g_c\big) \tag{3.6}$$

The first term $t(g_c)$ is the intensity distribution over $I(x, y)$ and contains no useful information. Thus, $t\big(g_0 - g_c, g_1 - g_c, \dots, g_{p-1} - g_c\big)$ or the second term can be used to model the local texture. This can also be written as:

$$t\left(s(g_0 - g_c), s(g_1 - g_c), \dots, s\big(g_{p-1} - g_c\big)\right) \tag{3.7}$$

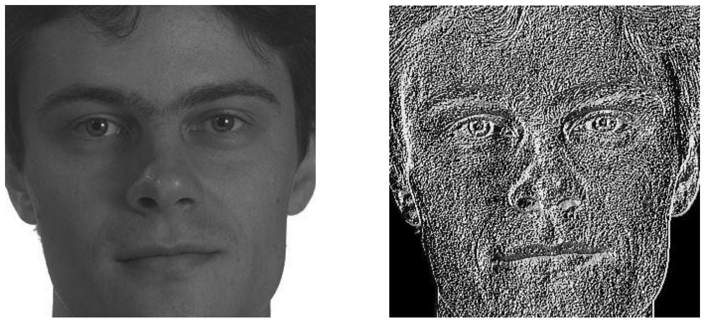
(a) (b)
Figure 3.6: Sample Image and its LBP Descriptor.

Where, s(z) is the thresholding (step) function

$$s(z) = \begin{cases} 0, & z < 0 \\ 1, & z \geq 0 \end{cases} \tag{3.8}$$

Thus,

$$LBP_{P,R}(x_c, y_c) = \sum_{p=0}^{p-1} s\big(g_p - g_c\big) 2^p \tag{3.9}$$

Hence, the signs of the differences in a neighborhood are interpreted as a P-bit binary number, resulting in 2^P distinct values for the LBP code.

$$T \approx t\left(LBP_{P,R}(x_c, y_c)\right) \tag{3.10}$$

A variation based on the local binary pattern descriptor is the Histogram of LBP. In order to compute this histogram, the LBP descriptor of the given image is found and then it is divided into non-overlapping $n_r\ X\ n_c$ blocks of same size, where,$n_r\ and\ n_c$ represent the number of rows and columns of blocks respectively. For each block, the histogram of local binary pattern is computed. These histograms are then normalized and concatenated into one large feature descriptor as shown in Figure 3.7.

The histograms provide three different levels of locality description of the image- pixel level information represented by histogram labels, regional level information represented by labels summed over a region, and global description which is built by concatenating the regional histograms. Thus, histogram of LBP provides information regarding the local micro patterns, such as edges, spots, etc. over the entire image. In [6] histogram of LBP is used for face authentication.

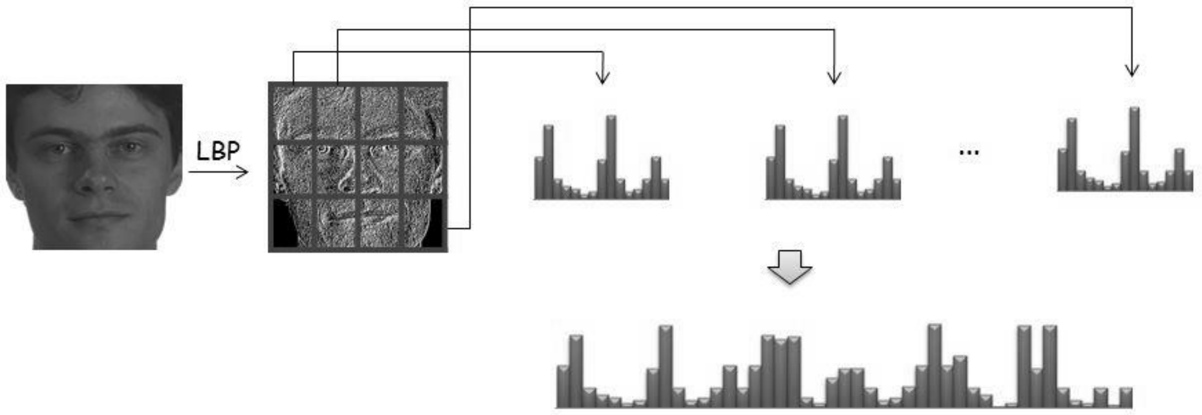

Figure 3.7: Process to create Histogram of LBP Descriptor.

3.5 BRISK & BRIEF Descriptors

BRIEF stands for Binary Robust Independent Elementary Features and was introduced in [28] by Calonder, Lepetit, Strecha and Fua. It is a simple binary descriptor which does not have any sampling pattern or an orientation compensation mechanism. Sampling pairs are chosen at any point in a patch and the descriptor is an n-dimensional bit string as shown in [28].

$$f_n(p) \coloneqq \sum_{1 \le i \le n} 2^{i-1}\, \tau(p; x_i, y_i) \tag{3.11}$$

$$\tau(p; x, y) \coloneqq \begin{cases} 1 & if\ p(x) < p(y) \\ 0 & otherwise \end{cases} \tag{3.12}$$

BRISK [10] is another binary descriptor which stands for Binary Robust Invariant Scalable Keypoints. It uses concentric rings as sampling pattern and uses this sampling pattern to find long and short pairs. It uses long pairs to determine the orientation and short pairs for intensity comparisons which builds the descriptor.

3.6 FREAK Descriptor

FREAK is a more sophisticated descriptor and outperforms other binary descriptors when there are viewpoint, rotation or illumination variations. It is more robust and it uses lower memory load [39].

The FREAK descriptor was introduced by Alahi, Ortiz and Vandergheynst [39]. This descriptor is inspired by the retina of human eye. It learns the sampling pairs by considering the pairs which are uncorrelated such that the resulting pairs match the model of the human retina. A circular retinal sampling grid is used which has high density of points near the center. Gaussian kernel is used in order to smooth each sampling point. Our eye tries to locate the object of interest first by using the peri-foveal receptive fields and then it performs the validation in the fovea using denser receptive fields. Similarly, FREAK first compares the sampling points in the outer region and then in the inner region. In order to make FREAK rotation invariant, the orientation of keypoint is measured and then the sampling pairs are rotated by that angle.

The belief that details from an image are extracted by human retina by using difference of Gaussians (DOG) of different sizes motivated the design of FREAK descriptor. In order to construct the descriptor, a circular retinal sampling grid is used with higher density of points near the center. Sampling points are smoothed in order to make it less sensitive to noise and every sampling point has a different kernel size to match it to retina model. Also, it uses overlapping receptive fields to increase performance.

The FREAK binary descriptor is constructed by using difference of Gaussians (DoG) with N size and P_a as the pair of receptive fields, as shown in equation below [39]

$$F = \sum_{0 \leq a \leq N} 2^a \, T(P_a) \tag{3.13}$$

$$T(P_a) = \begin{cases} 1 & if \ \left(I(P_a^{r_1}) - I(P_a^{r_2})\right) > 0 \\ 0 & otherwise \end{cases} \tag{3.14}$$

Where $I(P_a^{r_1})$is the smoothed intensity of the first receptive field of the pair P_a.

In this thesis, the FREAK descriptor was varied to form Histogram of FREAK descriptor. In order to compute Histogram of FREAK descriptor, the given image was divided into overlapping cells, such that these cells overlap by a fixed number of pixels. The FREAK descriptor is then found for all these cells with center of the cell as the keypoint. After that, for each of these keypoints, the histogram of their respective FREAK descriptor is computed. These histograms are then normalized and concatenated into one large feature descriptor as shown in Figure 3.8.

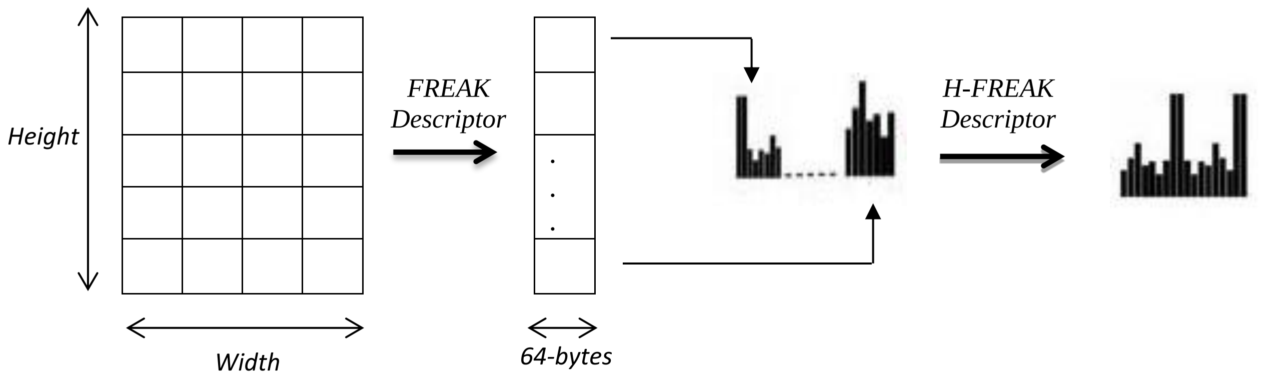

Figure 3.8: Process to create Histogram of FREAK Descriptor.

In the next chapter, fundamental concepts of dimensionality reduction are discussed.

Chapter 4

Dimensionality Reduction

Data in the real world generally can be very high dimensional. Working with high dimensional data can be computationally intensive and slow. In order to handle large amounts of such data, e.g. descriptors of digital images and video sequences, their dimensions need to be reduced. In cases where the feature space is extremely large, the effect known as the curse of dimensionality may result in lower performance compared to that of a lower dimensional feature space. The term "Curse of Dimensionality" was first introduced by Richard Bellman in 1961 [38] to refer to the problems caused by rapid increase in the data dimensions. A solution to this problem is to reduce the data by eliminating the dimensions that seem irrelevant. Thus, the aim of dimensionality reduction is to transform the high dimensional data to a lower dimensional space while retaining the important properties of the data for the problem under consideration. Dimensionality reduction offers computational benefits obtained by processing a smaller amount of data. A secondary benefit of dimensionality reduction is that some noise and redundancies in the features are eliminated after reducing the feature space. As a result, the data can be represented in a more compact and effective way, which can improve classifier performance. Techniques such as Principal Component Analysis (PCA), Linear Discriminant Analysis (LDA), and Manifold Learning have been used for subspace learning and dimensionality reduction [12].

More formally, we let the input feature space contain n samples $x_1, x_2, \ldots, x_n$, each of D dimensions. These n samples need to be projected onto a lower dimensional space Y which has dimensions $d \ll D$. Thus, the samples are transformed to $y_1, y_2, \ldots, y_n$, each of dimension d. In matrix notation, the input feature space X, is described by $n\ X\ D$, where the i^{th} row represents input sample x_i and i^{th} column represents the i^{th} feature. Hence, the lower dimensional feature matrix is given as, $Y = X * A$, with dimensions $n\ X\ d$ and A is the transformation matrix.

4.1 Principal Component Analysis

Principal Component Analysis was first introduced by Pearson in 1901 and is the most often used dimensionality reduction method. Principal component analysis (PCA) transforms the data dimensions by retaining the first few principal components, which account for most of the variation in the original data. PCA is a well-established and effective technique, but it has the limitation of requiring knowledge of the data statistics.

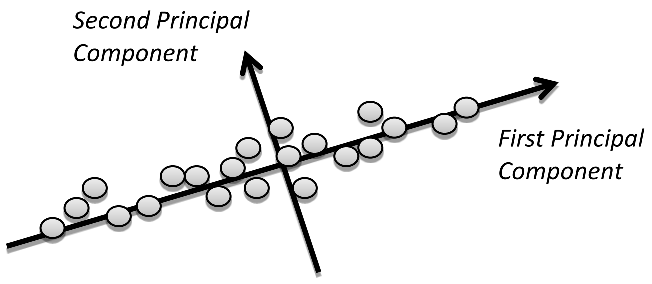

Figure 4.1: Principal Components of an Example Data.

Let $x_1, x_2, \dots, x_n$ be the original set of data in D dimensional space and let $y_i;\ i = 1, \dots n$ be the representation of this data into some subspace Y which has dimension $d < D$ such that the reconstruction error given in Equation (4.1) is minimum, where μ is the mean and A is a $D \times d$ matrix with d orthonormal vectors.

$$\min_{\mu, x_{1 \dots n}, v_d} \sum_{i=1}^{n} \|y_i - \mu - Ax_i\| \tag{4.1}$$

PCA finds a linear projection of high dimensional data into a lower dimensional subspace such that the variance retained is maximized and the least square reconstruction error is minimized, i.e.

$$e_1 = \ argmax_{e_i} \ var(xe_1) \\ Subject\ to: e_1^T e_1 = 1 \tag{4.2}$$

Rewriting in terms of covariance matrix, we get

$$var(xe_1) = \ var(y_1) = \ e_1^T \Sigma e_1 = \ \lambda_1 \tag{4.3}$$

Where, Σ is the covariance matrix of x and λ_1 is the largest eigenvalue. In general

$$var(xe_k) = \ var(y_k) = \ e_k^T \Sigma e_k = \ \lambda_k \tag{4.4}$$

Where λ_k is the k^{th} largest eigenvalue of Σ.

In matrix notation,

$$y = \ A^T(x - m_x) \tag{4.5}$$

Where, $A = [\ e_1| \ldots |e_n]$ is the matrix whose columns are the eigenvectors of Σ, the covariance of the original data, and m_x is the mean of the original data.

When the mean and covariance of the testing samples do not accurately match these of the training data, this approach could lead to errors.

4.2 Random Projections

Random Projection is another linear dimensionality reduction technique. It is based on the Johnson-Lindenstrauss (JL) lemma [14] which states that for a set of points of size *n* in *D*-

dimensional Euclidean space there exists a linear transformation $y = \boldsymbol{R}x$ of the data into a *d*-dimensional space, $d \geq O(log(n)/\varepsilon^2)$, that preserves distances up to a factor of $1 \pm \in$ and for all *x*, *y*:

$$(1-\varepsilon)\sqrt{d/_D} \leq \frac{\|\boldsymbol{R}x - \boldsymbol{R}y\|_2}{\|x-y\|_2} \leq (1+\varepsilon)\sqrt{d/_D} \tag{4.6}$$

The random matrix $\boldsymbol{R} \in \mathbb{R}^{d \times D}$ has elements that are drawn as independent, identically distributed (i.i.d) samples from a zero mean distribution with bounded variance. Random Projection transformation preserves distances, within some bounds, in the reduced dimensional space.

From the implementation perspective, there exists a computationally efficient method for computing the projection matrices of the RP transformation. In [38] it was shown that the elements r_{ij} of $\boldsymbol{R}$ can be drawn i.i.d from either of the following distributions:

$$r_{ij} = \begin{cases} +1 \; with\, probability \; 1/2 \\ -1 \; with\, probability \; 1/2 \end{cases} \tag{4.7}$$

or

$$r_{ij} = \sqrt{3}. \begin{cases} +1 \; with\, probability \; 1/6 \\ \;\; 0 \; with\, probability \; 2/3 \\ -1 \; with\, probability \; 1/6 \end{cases} \tag{4.8}$$

The transformation based on an RP matrix with coefficients following Equation (4.8) is particularly efficient, since it discards 2/3 of the data that correspond to multiplication by zero. Furthermore, if the scaling coefficient is factored out, the transformation can be implemented using fixed point arithmetic operations consisting of only additions and subtractions.

There are some notable advantages to using RP transformations for dimensionality reduction. Both PCA and RPs involve linear transformations and thus offer fast application through matrix multiplications. The nature of the RP projection matrix is such that the computations are more efficient as the RP matrix consists of zeroes and ones. Furthermore, unlike PCA, RPs is data-independent, i.e. it is does not require training on a particular dataset and thus allows better generalization.

4.3 Manifold Learning

There may be cases when linear dimensionality reduction techniques such as PCA, RP, etc, might not be adequate for capturing the data structure into lower dimensional space. For example, the lower dimensional data space may not reside on a Euclidean data space but instead may be on a non-linear manifold. A manifold is a topological space in which each point has a neighborhood that is homeomorphic to a Euclidean space. Homeomorphism between two geometrical objects or topological spaces is a continuous stretching or bending of one object or space into other space or object. There are various algorithms for manifold learning such as Isomap [60], Locally Linear Embedding, and Laplacian Eigenmaps [61]. These algorithms model the given data by a weighted adjacency graph with input samples as vertices and the edges represent the proximity between vertices.

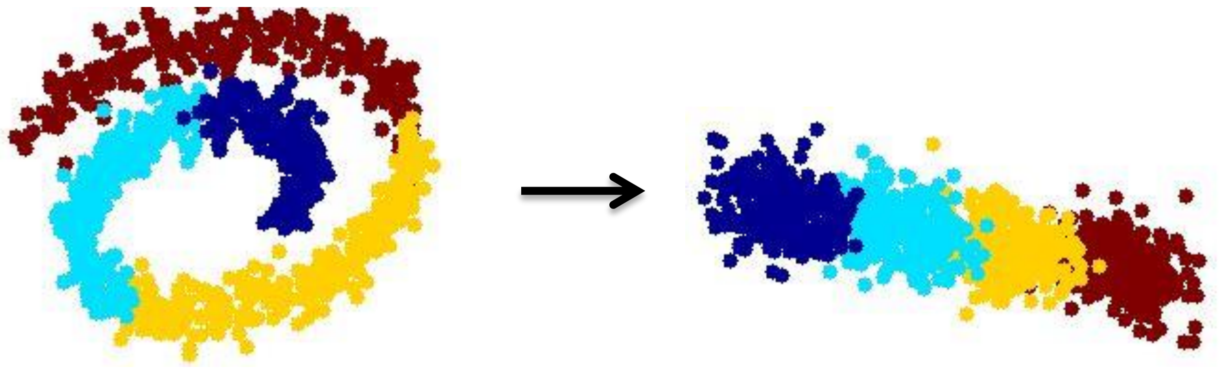

Figure 4.2: Manifold to Euclidean Space.

4.4 Locality Preserving Projections (LPP)

The linear dimensionality reduction methods such as PCA, RP, etc. are adequate when the given data is linear whereas non-linear dimensionality reduction methods such as Isomaps, LLE, etc. perform better when dealing with non-linear data. Linear methods have their limitations as most of the real world datasets are highly non-linear, whereas non-linear dimensionality reduction techniques are computationally complex as compared to the linear dimensionality reduction techniques. Locality Preserving Projection is a linear method of dimensionality reduction and it aims at preserving the local manifold structure of the given data while transforming them into a new space and was introduced by He and Niypgi in [15]. It builds a graph incorporating the neighborhood information of the data and then finds a linear transformation matrix which is used to transform the high dimensional data to a lower dimensional space.

The algorithm described in [15] is as follows. Given a set $x_1, x_2, \dots, x_m \; in \; \mathbb{R}^D$, we need to find a transformation matrix A which maps these m points to a set of points $y_1, y_2, \dots, y_m \; in \; \mathbb{R}^d$ $(d \ll D)$ such that

$$y_i = A^T x_i \tag{4.9}$$

1. Construct an Adjacency graph: Let G be a graph with m nodes and there is an edge between nodes *i* and *j* if x_i and x_j are close to each other. There are two variations:
    a. Є-neighborhoods (parameter $\mathcal{E} \in \mathbb{R}$): Nodes *i* and *j* are connected by an edge if $\left\|x_i - x_j\right\|^2 < E$, where the norm is Euclidean norm in $\mathbb{R}^n$.
    b. k-nearest neighbors (parameter $\in N$): Nodes *i* and *j* are connected by an edge if *i* is among *k* nearest neighbors of *j* or vice versa.

2. Choosing the weights: W is a sparse symmetric $m \times m$ matrix with W_{ij} having the weight of the edge joining vertices i and j , and 0 is there is no such edge.
    a. Heat Kernel (parameter $t \in \mathbb{R}$): If nodes i and j are connected, then

    $$W_{ij} = \exp\left(-\left\|x_i - x_j\right\|^2/t\right)$$

    b. Simple-minded (no parameter): $W_{ij} = 1$ if and only if vertices i and j are connected by an edge.
3. Eigenmaps: Eigenvectors and eigenvalues are then computed.

$$XLX^T a = \lambda XDX^T a \tag{4.10}$$

Where D is a diagonal matrix whose entries are column (or row, since W is symmetric) sums of W, $D_{ii} = \Sigma_j W_{ji}$. L=D-W is the Laplacian matrix. The i^{th} column of matrix X is x_i.

Thus, $A = [\ \alpha_1|\ ...\ |\alpha_d]$, where column vectors $\alpha_1, \alpha_2\ ...\ \alpha_d$ are the solutions of Equation (4.10).

LPP preserves the local structure of the data whereas PCA preserves the global structure. Since, locality preserving projection is linear approximation of non-linear dimensionality reduction methods; it can preserve the intrinsic non-linear manifold structure of the datasets and can be used as an alternative to PCA.

Next chapter discusses the concept of classification.

Chapter 5

Classification

In the world today there exists a large variety of data and this data is collected and recorded on every aspect of human endeavor. Banking, communication, the internet, visual information, etc., are various examples of such aspects. Thus, to be able to make sense of any of these domains, the ability to process and interpret a large amount of data is required. Classification is the problem of automatically assigning an object to one of several (often pre-defined) categories based on the attributes of the object.

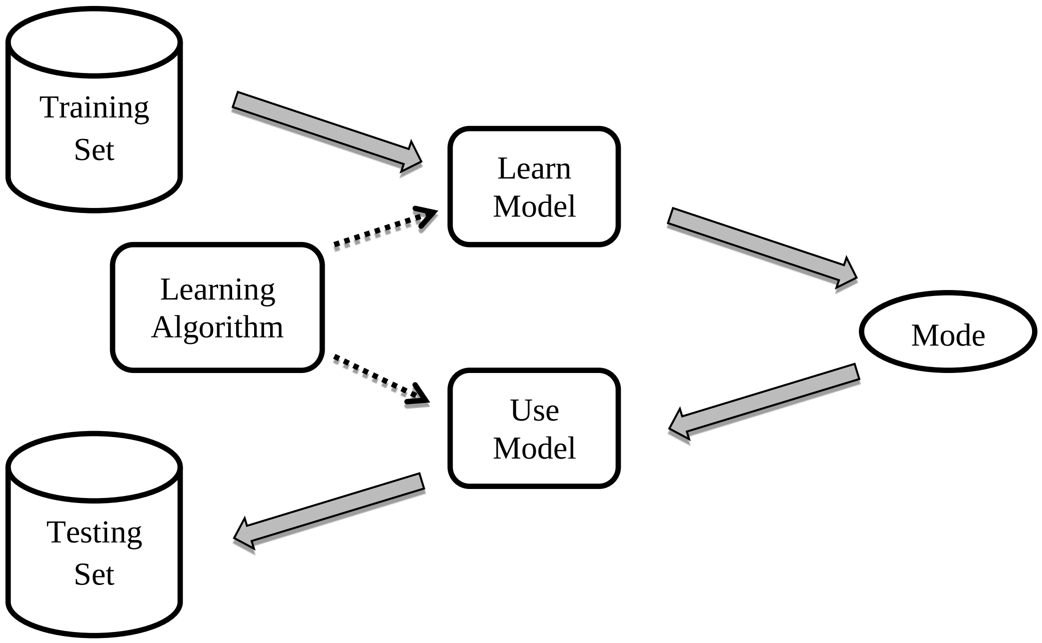

Figure 5.1: Classification Example.

In the classification problem we are generally given a training set of objects and their attributes are called features. Along with this we are given the categories or class labels of each object. A classifier is then constructed based on the training set. When a training dataset has class labels, it is known as supervised classification. There are several methods of classification, example support vector machines, nearest neighbors, decision trees, neural networks, etc.

Classification is a two-step process as shown in Figure 5.1. First step is model construction. Model construction describes a set of predetermined classes. Each sample in this is assumed to belong to a predefined class, as determined by the class label attribute. The model is represented as classification rules, etc. The second step is model usage. This step is used for classifying future or unknown objects.

5.1 Support Vector Machines

The Support Vector Machine (SVM) was first introduced by Boser, Guyon and Vapnik in [43] and since then, it is very popular due to its simplicity and excellent performance. SVM was developed from Statistical Learning Theory. It is a supervised learning algorithm which is used for classification and regression and belongs to the family of generalized linear classifiers.

5.1.1 Statistical Learning Theory

Statistical learning theory models data as a function estimation problem and is described as a system that receives some data as input and outputs a function that can be used to predict some features of future data. Thus, a set of training patterns or the training data $\{(x_1, y_1), (x_2, y_2), \dots, (x_n, y_n)\}$ is given, where x_i is the i^{th} training sample and y_i is the class label associated with i^{th} training sample. Thus, SVM finds an optimal separating hyperplane or the hypothesis that is able to correctly classify the given training data.

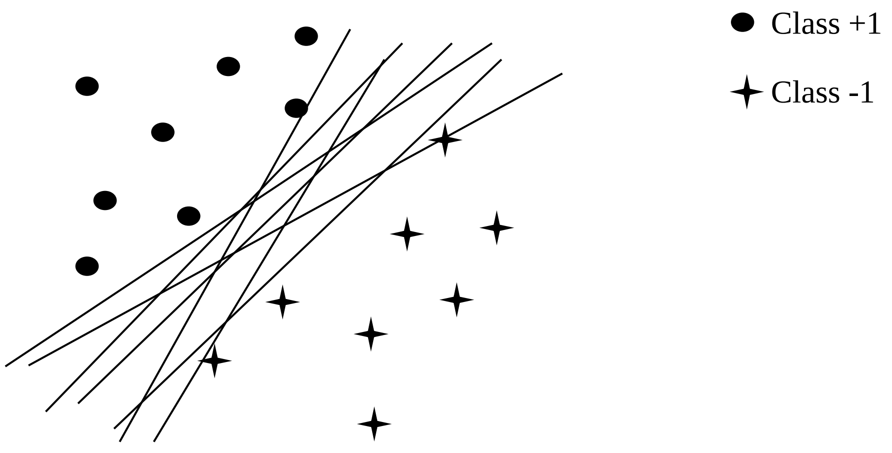

Figure 5.2: Two Class Classification Example using Support Vector Machine.

As seen from Figure 5.2 there could be many hyperplanes which can classify a given set of data. However, there is only one of these that achieve the maximum separation. SVM finds an optimal separating hyperplane that maximizes the margin, where margin is the distance between support vectors and the support vectors are the examples closest to the hyperplane.

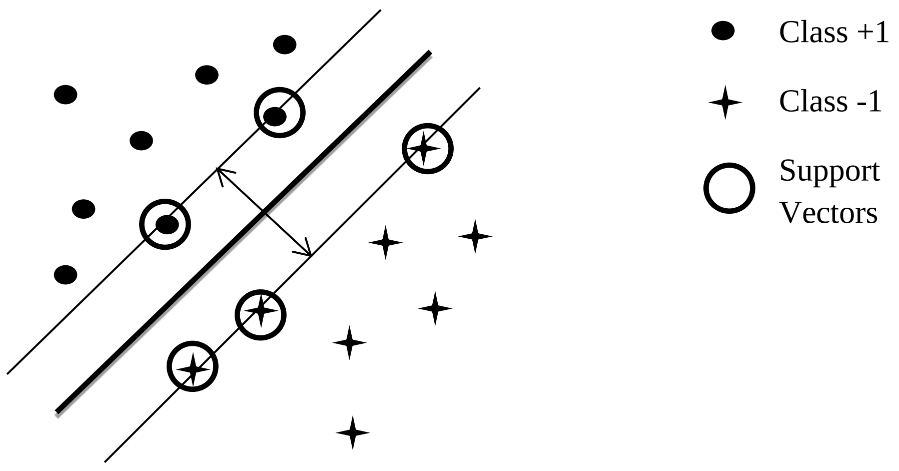

Figure 5.3: Example to show Support Vectors, Margin and Decision Boundary.

5.1.2 SVM Mathematical Representation

Let there be a set of training patterns $\{ x_i ; i = 1, \; \dots, n\}$ assigned to one of the two classes ω_1 and ω_2, with labels $y_i = \; \pm 1$ are given, such that

$$For\ y_i = +1, \quad w^T x_i + b > 0 \tag{5.1}$$

$$For\ y_i = -1, \quad w^T x_i + b < 0 \tag{5.2}$$

Where, *w* is the parameter vector and *b* is the offset vector. Thus for all training samples,

$$y_i(w^T x_i + b) \; \geq 1 \tag{5.3}$$

To classify the given dataset, we need to find a linear discriminant function, or decision boundary such that

$$g(x) = \; w^T x + b = 0 \tag{5.4}$$

This desired hyperplane which maximizes the margin also bisects the lines between closest points on convex hull of the two datasets. The distance of a closest point on a hyperplane to the origin can be found by maximizing *x*, as *x* is on the hyperplane. Similarly for points on the other side, we have a similar scenario. Thus, solving and subtracting the two distances we get the summed distance from the separating hyperplane to nearest points. Maximum Margin = M = 2 / ||w||

In order to maximize the margin, we need to find a solution that minimizes the ||w||, subject to constraints

$$y_i(w^T x_i + b) \geq 1 \quad for\ i = 1 \ldots n \tag{5.5}$$

This leads to a quadratic optimization problem with linear constraints. The solution involves determining the saddle point of function using Lagrange multipliers

$$L_p = \frac{1}{2} w^T w - \sum_{i=1}^{n} \alpha_i (y_i(w^T x_i + b) - 1) \tag{5.6}$$

Where $\alpha_i \geq 0$

$$\frac{\partial L_p}{\partial w} = 0 \Rightarrow w = \sum_{i=1}^{n} \alpha_i y_i x_i \tag{5.7}$$

$$\frac{\partial L_p}{\partial b} = 0 \Rightarrow \sum_{i=1}^{n} \alpha_i y_i = 0 \tag{5.8}$$

Since, only the support vectors have $\alpha_i \neq 0$

The solution has the form

$$w = \sum_{i=1}^{n} \alpha_i y_i x_i = \sum_{i \in SV} \alpha_i y_i x_i \tag{5.9}$$

And b can be found using $y_i(w^T x_i + b) - 1 = 0$ where x_i is the support vector.

Thus, the decision rule is given as

$$g(x_i) = w^T x_i + b = \begin{cases} > 0 \\ < 0 \end{cases} \Rightarrow x_i \in \begin{cases} \omega_1;\ y_i = +1 \\ \omega_2;\ y_i = -1 \end{cases} \tag{5.10}$$

5.1.3 Non Linear SVM

For linear data, a separating hyperplane may be used to classify the data. However, often the data is non-linear. To classify a non-linear dataset, the input data is mapped to another high dimensional feature space where the data is linearly separable.

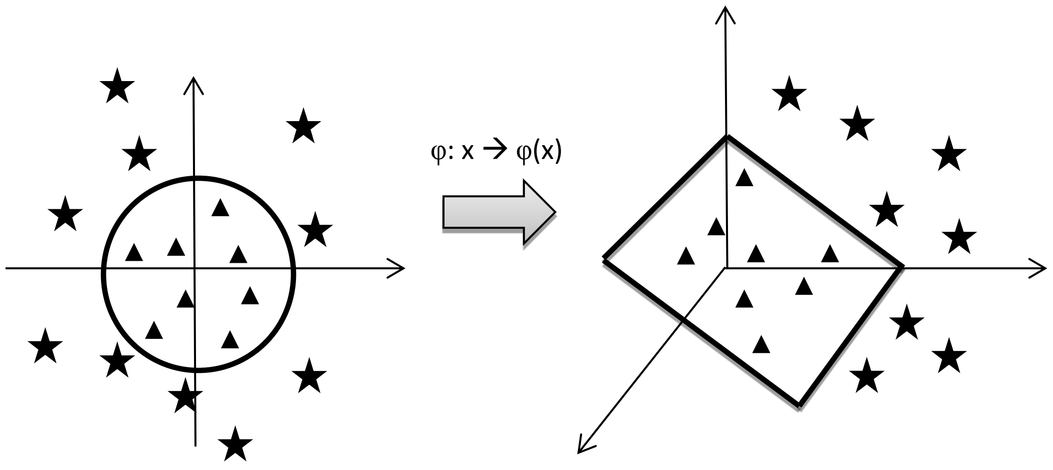

Figure 5.4: Non-Linear Classification using SVM.

If the feature space is chosen suitably, classification can be easy. This is also known as the Kernel trick and the mapping is defined by the kernel

$$K(x,y) = \varphi(x).\varphi(y) \tag{5.11}$$

Thus, the data is mapped or transformed to a higher dimensional feature space and then the hyperplane is constructed in that feature space such that all other above equations are the same. Thus, the decision rule is given as

$$g(\varphi(x_i)) = w^T K(x,y) + b = \begin{cases} > 0 \\ < 0 \end{cases} \Rightarrow x_i \in \begin{cases} \omega_1;\ y_i = +1 \\ \omega_2;\ y_i = -1 \end{cases} \tag{5.12}$$

This is known as the Kernel Trick. Some of the kernel functions are:

- Polynomial – $K(x, y) = (\langle x, y\rangle + c)^d$ where c, d are constants
- Gaussian Radial Basis Function – $K(x, y) = \exp\left(-\frac{\|x-y\|^2}{2\sigma^2}\right)$
- Exponential Radial Basis Function – $K(x, y) = \exp\left(-\frac{\|x-y\|}{2\sigma^2}\right)$
- Multi-Layer Perceptron – $K(x, y) = \tanh(\rho\langle x, y\rangle + c)$

5.1.4 Multiclass SVM

SVM is a binary classifier in which there can be only two classes. However, in most of the real world problems like handwritten digit classification, optical character recognition, etc. there are more than two classes. Thus, in multiclass SVM, each training point belongs to one of C different classes and the goal is to construct a function which, given a new data point, will correctly predict the class to which the new point belongs.

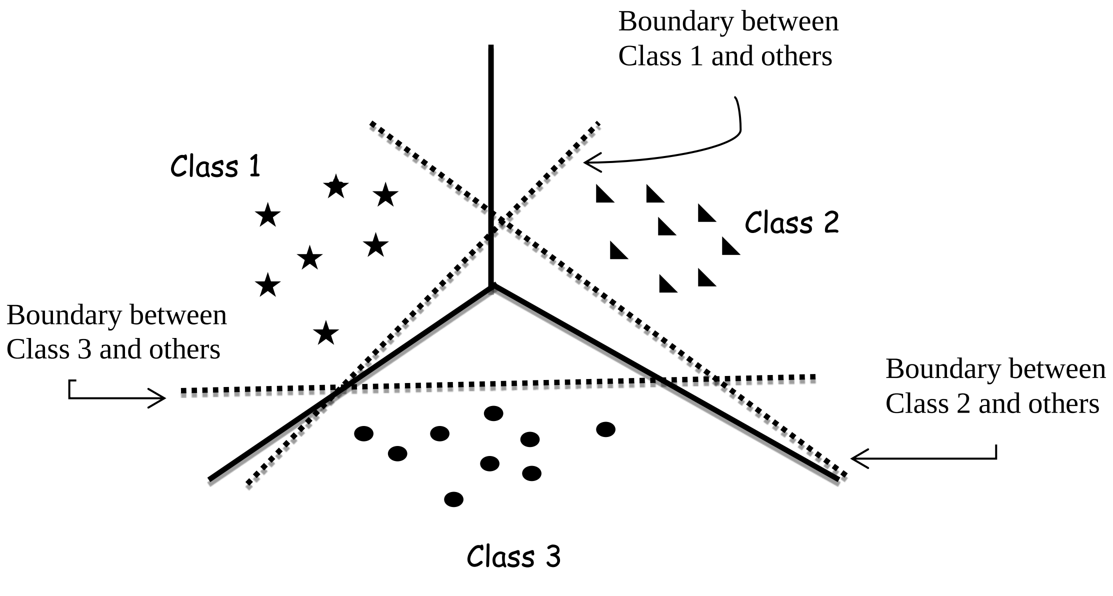

Figure 5.5: Multi-class Classification using SVM.

In order to solve a multiclass classification problem, C different binary classifiers are built and each of these classifiers is built to separate one class from the others. These N classifiers are then combined to get a multi-class classifier. Thus, for the i^{th} classifier, the positive examples are all the samples in class *i*, and the negative examples are all the samples which are not in class *i*.

5.2 Bootstrapping

The term bootstrapping came from "pulling oneself up by the strap of the boot" in early 19th century. It is a method to incrementally train a classifier from a large set of training set of samples. In order to train a classifier it is good to have as many training samples as possible, but there are many limitations to having a large set of training data, such as storage or computation resources.

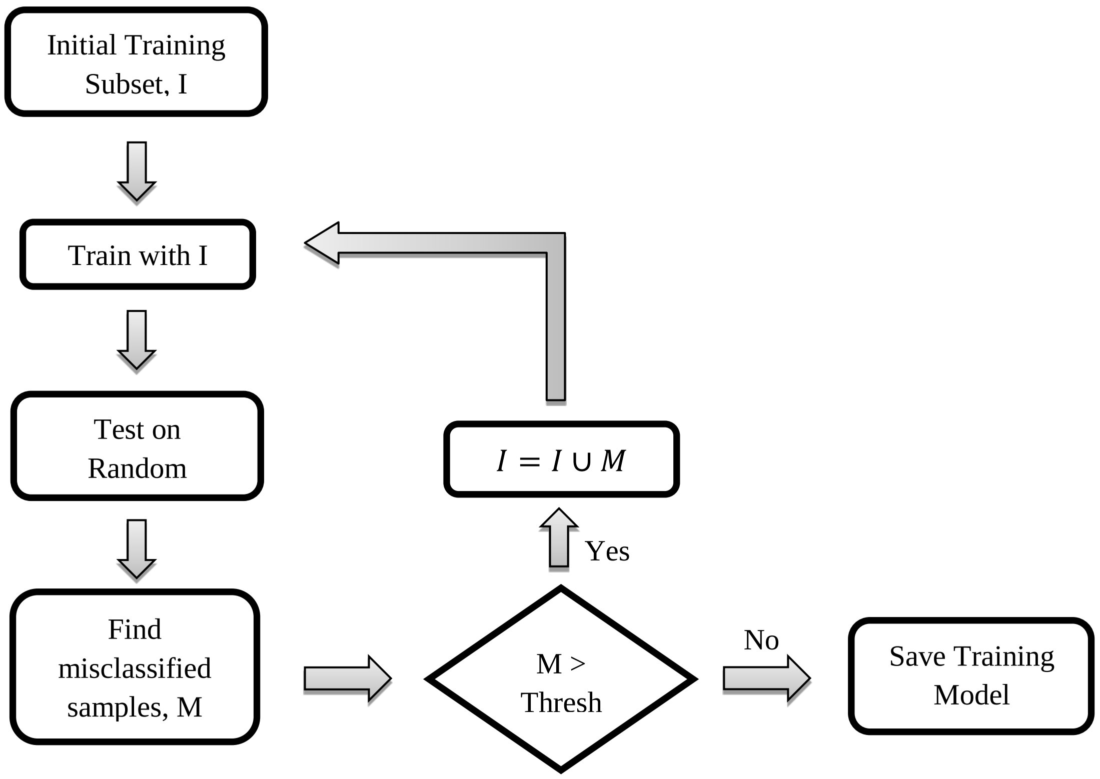

Figure 5.6: Flowchart for Bootstrapping Algorithm.

Collecting object or positive class samples is easier as there could be a limited number of samples for objects. But, collecting non object or negative class samples could be trickier as every image patch that does not contain the object can be added to the negative class sample. This may result in an exhaustively large set of samples. Thus, in order to restrict the amount of data samples in the negative class category, we use the “bootstrapping” algorithm which selects only the required non object patterns from a given training set.

It is an iterative algorithm in which the classifier is given an initial set of random samples from the large training set. In order to improve the performance, the misclassified samples are added to the initial training set and the classifier is retrained. The algorithm is as shown in Figure 5.6.

5.3 SVM Usage

In this thesis, we use the LIBSVM [58] library for support vector machine classification. Support vector machines were preferred over other methods as they aim to maximize the distance between the positive class and negative training samples. Support vector machines also give the option of various different kinds of kernels which can be used to improve the classification performance.

In training, initial positive and negative training data are extracted by using the location of the object of interest, as provided by the training dataset. The negative training examples are extracted by using random windows that do not contain the object. There can be many such windows and it is not always possible to store all the negative training examples and thus the bootstrapping technique was used to collect only the samples which are relevant and hence help in learning a stronger classifier.

Chapter 6

Eye Detection

6.1 Motivation

With the proliferation of webcams and mobile devices, eye detection is becoming increasingly important for human computer interaction and augmented reality applications. Human eyes play an important role in face detection/recognition, face tracking, facial expression recognition. In the context of mobile interfaces, eye detection provides cues on whether or not the user is looking at the screen [20]. Furthermore, eye detection is the starting point for gaze estimation and eye tracking. Following face detection, eye locations can be used for face alignment, normalization, pose estimation, or initial placement of Active Shape/Active Appearance Models for efficient convergence. Several eye detection systems are relying on infrared light emitting diodes, but in general it cannot be assumed that such devices are available.

Eyes are the most prominent facial feature and their localization has received considerable attention in the computer vision literature. Eye detection methods include active approaches that require infrared illumination [21], model-based approaches, such as active shape models [22], methods based on geometrical features, such as eye corners or iris detection [23], and methods based on feature classification [24], for example using Support Vector Machine (SVM) classifiers. Methods relying on corners or circles are susceptible to noise, low resolution or poor illumination. Active Shape models require good initialization and may be computationally intensive. In this thesis, we consider a computationally efficient approached to eye detection.

6.2 Approach

In this work, a robust and efficient eye detector operating on images or video was developed based on feature classification using Support Vector Machines. The overall eye detection system is shown in Figure 6.1. The left path in the diagram outlines the training process, while the right path outlines the testing process.

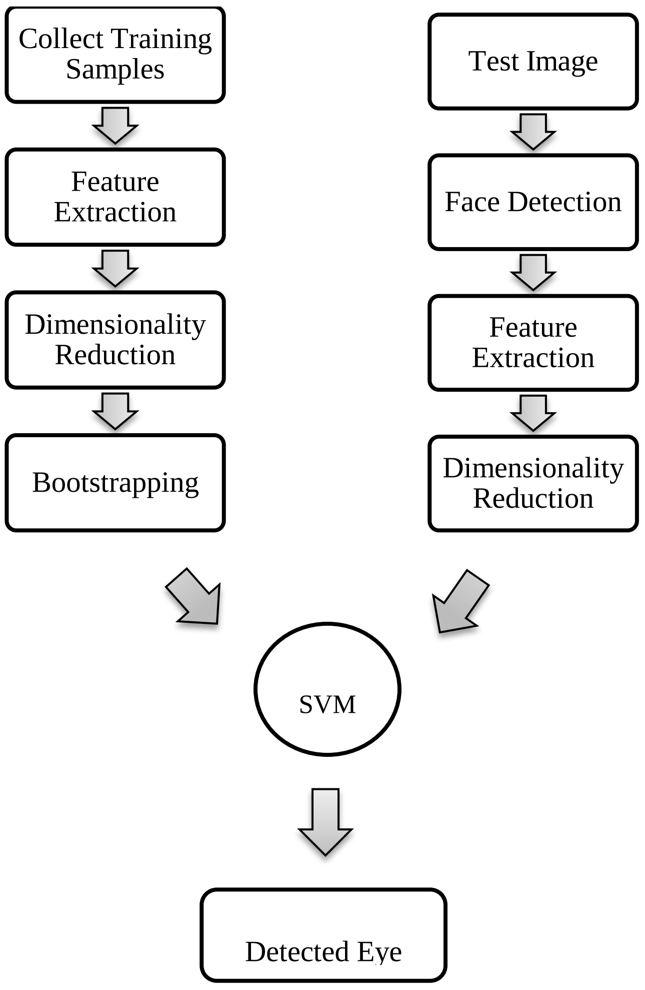

Figure 6.1: Eye Detection System.

In order to train the SVM classifier, different eye and non-eye patches were collected from the BioID and FERET [50] databases as shown in Figure 6.2. A feature descriptor was computed for all these patches. In order to make the descriptor computationally efficient and improve the classification performance, dimensionality reduction techniques were used to reduce the number of features.

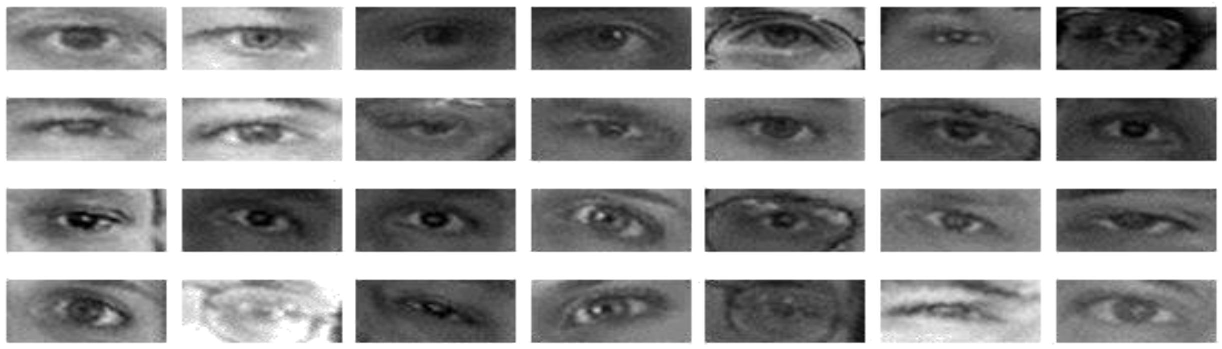
(a)

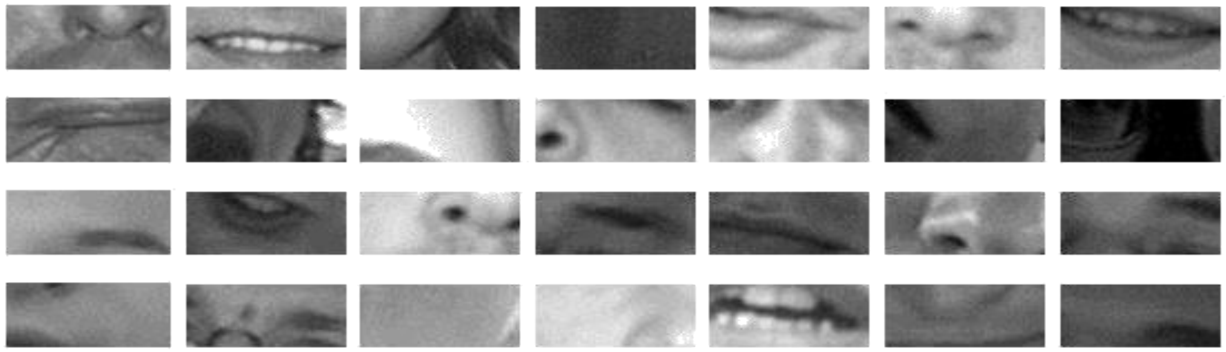
(b)

Figure 6.2: Example (a) Eye and (b) Non-Eye Training Samples.

During the final stage of testing, the bootstrap technique [56] was used to reduce the number of false positives. The bootstrapping method was performed as follows:

a) A subset of samples was taken from the original training set and the classifier was trained on this subset.
b) This classifier was tested on a random subset of samples.
c) If the number of false positives were less than the specified threshold, the algorithm was stopped.

d) Otherwise, the false positives were added to the training set, a new classifier was trained and step b) was repeated.

To test the eye detector on a face image, a sliding window of varying size is used for extracting image patches for feature extraction and classification. This process can be computationally intensive and thus is combined with face detection to reduce the search area for faster processing. A face detector based on the Viola-Jones detector [57] is used to identify the face region. After face detection, the face region is normalized to a standard size and the local windows for eye detection are extracted from the upper portion of the face region. The feature descriptor is computed for each local window and a linear SVM classifier is used to classify the patches into eyes or non-eyes. After identifying the top 5 patches that are classified as eyes based on the probability estimates, i.e. probability that the testing instance is in a class, (returned by the LIBSVM [58] classifier), we cluster them to determine the location of the eye.

Chapter 7

Experimental Results and Discussion

7.1 Datasets

7.1.1 BioID

The results were evaluated using the BioID Face Database and the FERET Database. The BioID database consists of 1521 frontal images of 23 different persons. The images are grayscale and have size 384x286 pixels. The database includes annotations of 20 locations of facial feature points for each image.

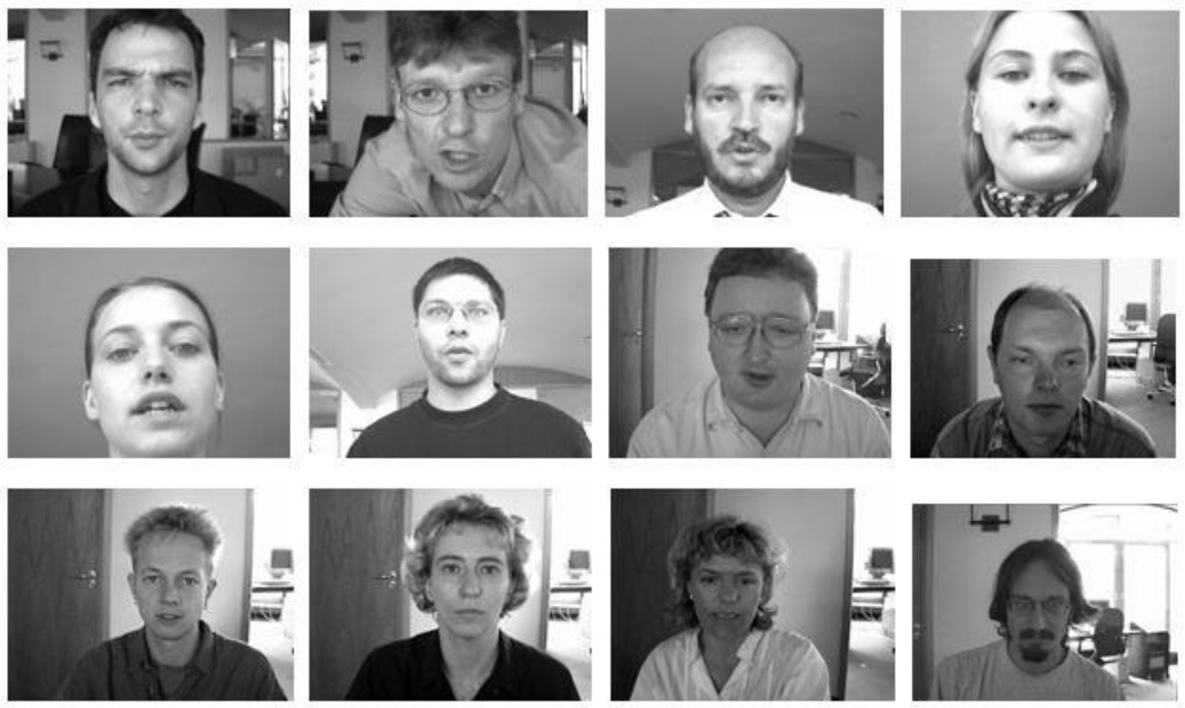

Figure 7.1: Example Images from BioID.

7.1.2 FERET

The FERET database contains both frontal as well as posed faces. The database contains 1564 sets of images with 365 duplicate sets. The duplicate sets contain images of a person already in the database, but taken on a different day. For some individuals, the time elapsed between their first and last sitting was over a year in order to accommodate the changes in appearance over time.

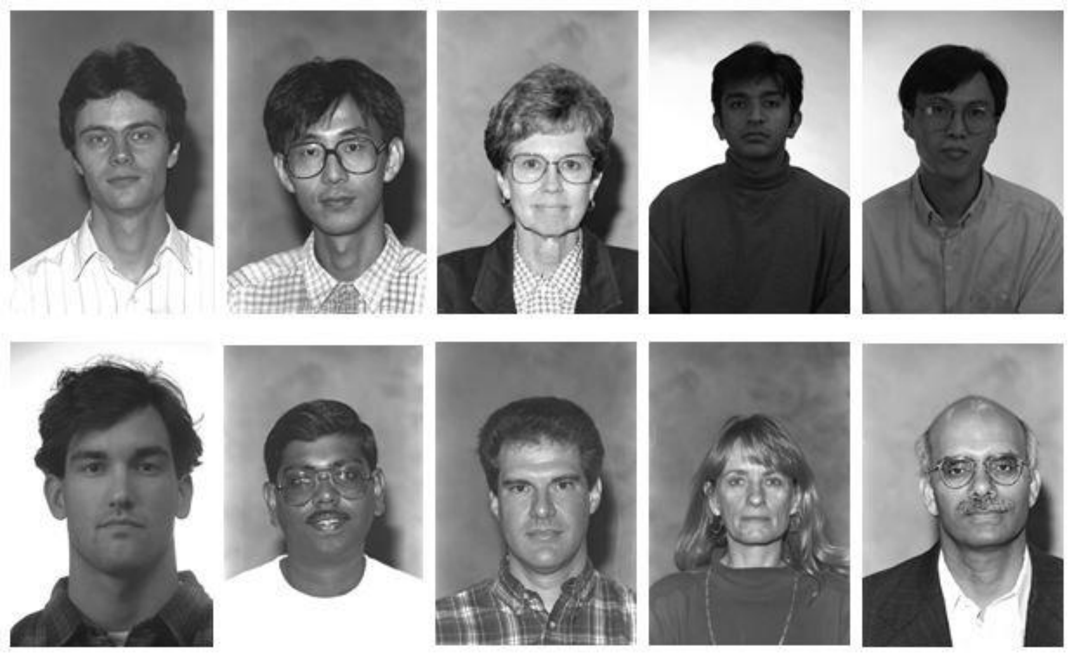

Figure 7.2: Example Images from FERET.

7.1.3 CalTech-101

The CalTech-101 dataset consists of 102 object categories and each category consists of 31 to 800 images per category. These are colored images with size around 300 x 200 pixels. Additionally, an outline of each object is provided. Figure 7.3 shows some example images from CalTech-101.

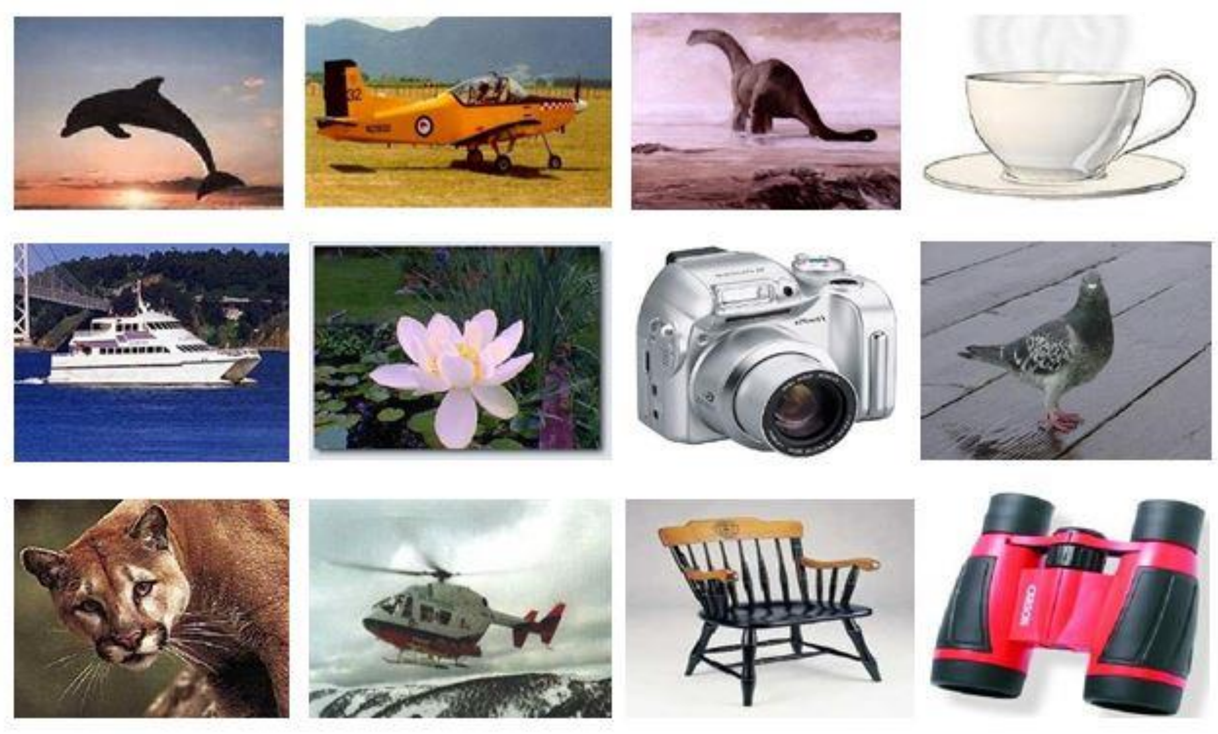

Figure 7.3: Example Images from CalTech-101.

7.2 Eye Detection

The training set consisted of 8,258 eye samples and 9,836 non-eye samples extracted from the BioID and FERET databases. The extracted eye and non-eye patches were normalized to compensate for variations in illumination. The classification performance was tested using 10-fold cross validation technique. Figure 7.4 shows accuracy results and Figure 7.5 shows false positives of eye detection with various image descriptors and dimensionality reduction techniques. Table 7.1 shows accuracy results with different SVM kernels.

Table 7.1: Accuracy Results with HOG and different SVM Kernels.

Kernels	***Linear***	***Radial Basis***	***Sigmoid***
Accuracy	98.91	97.82	97.59

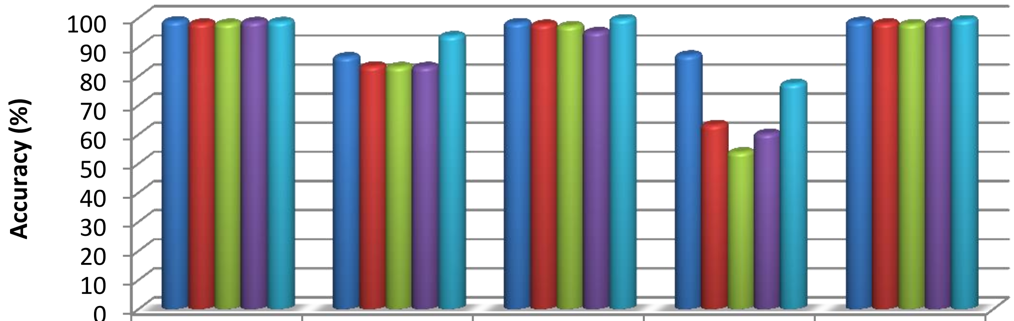

	HoG	FREAK	H-FREAK	LBP	H-LBP
🟦 Orignal	98.91	86.59	98.3	87.18	98.74
🟥 PCA	98.16	83.42	97.77	63.29	98.19
🟩 RP	98.11	83.22	97.24	53.92	97.92
🟪 LPP	98.71	83.22	95.22	60.26	98.47
🟦 SLPP	98.7	93.84	99.62	77.42	99.28

Figure 7.4: Eye Detection Accuracy Results with different Descriptors and Dimensionality Reduction methodologies.

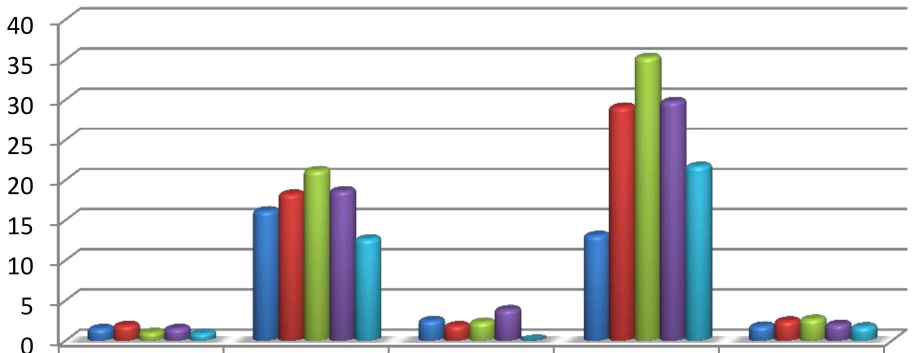

	HoG	FREAK	H-FREAK	LBP	H-LBP
🟦 Orignal	1.52	16.17	2.51	13.12	1.82
🟥 PCA	1.91	18.26	1.87	29.09	2.45
🟩 RP	1.03	21.19	2.3	35.29	2.69
🟪 LPP	1.53	18.67	3.87	29.79	2.03
🟦 SLPP	0.91	12.67	0.03	21.73	1.73

Figure 7.5: Eye Detection False Positives with different Descriptors and Dimensionality Reduction methodologies.

HOG Descriptor

The HOG descriptor was found using the cell size as 8, block size as 2 and bin size as 9. Thus, the descriptor length was found to be 648 for patch size of 25 x 50 and this was reduced to 130 (20%) using different dimensionality reduction techniques. Tables 7.2-7.6 show the confusion matrices with Histogram of Oriented descriptor.

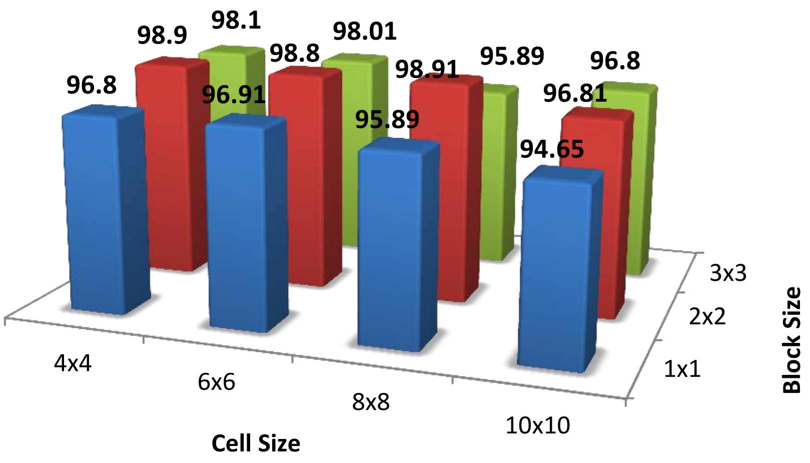

Figure 7.6: Detection Accuracy as Cell Size and Block Size were varied.

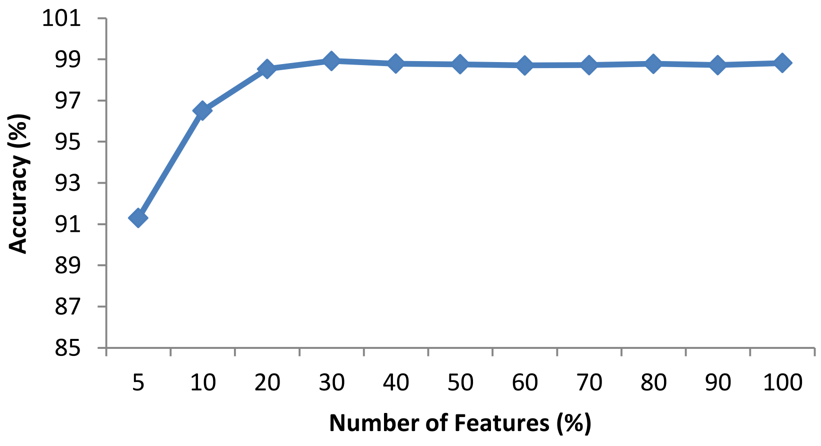

Figure 7.7: Accuracy as Number of Features is varied.

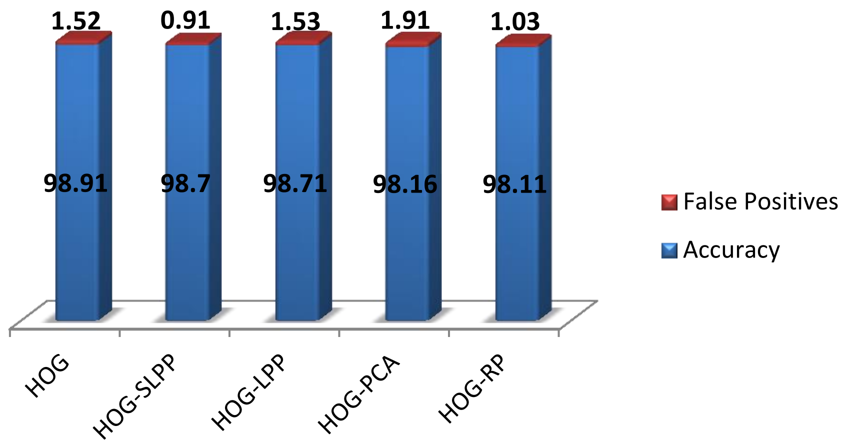

Figure 7.8: Accuracy and False Positives with Histogram of Oriented Gradients.

Table 7.2: Confusion Matrix for Eye Detection using HOG Descriptor.

	Eyes	***Non Eyes***
Eyes	98.91	1.09
Non Eyes	1.52	98.48

Table 7.3: Confusion Matrix for Eye Detection using HOG –PCA Descriptor.

	Eyes	***Non Eyes***
Eyes	98.16	1.84
Non Eyes	1.91	98.09

Table 7.4: Confusion Matrix for Eye Detection using HOG-RP Descriptor.

	Eyes	***Non Eyes***
Eyes	98.11	1.89
Non Eyes	1.03	98.97

Table 7.5: Confusion Matrix for Eye Detection using HOG – LPP Descriptor.

	Eyes	***Non Eyes***
Eyes	98.71	1.29
Non Eyes	1.53	98.47

Table 7.6: Confusion Matrix for Eye Detection using HOG – SLPP Descriptor.

	Eyes	***Non Eyes***
Eyes	98.7	1.3
Non Eyes	0.91	99.09

FREAK Descriptor

The FREAK descriptor was computed in Matlab using the inbuilt function with radius 21. Since, the radius of the descriptor was fixed; the patch size was made as 50 x 50 in order to match the radius. The descriptor length was found to be 512 and was reduced to 102 using different dimensionality reduction techniques. Tables 7.7-7.11 show the confusion matrices with FREAK descriptor.

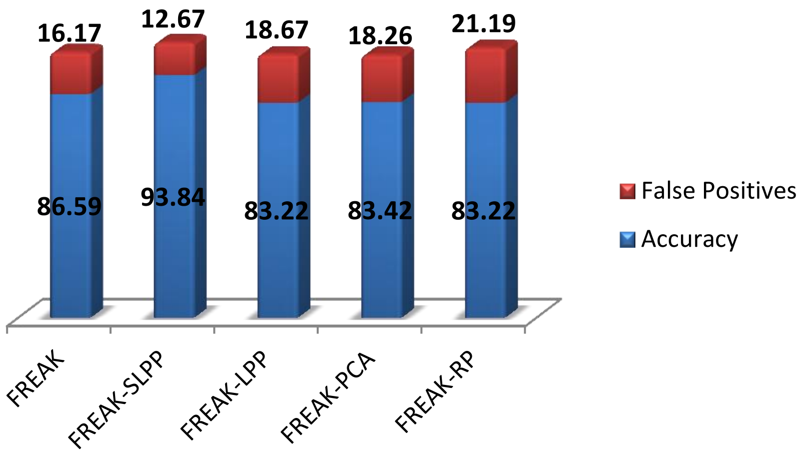

Figure 7.9: Accuracy and False Positives with FREAK.

Table 7.7: Confusion Matrix for Eye Detection using FREAK Descriptor.

	Eyes	***Non Eyes***
Eyes	86.59	13.41
Non Eyes	16.17	83.83

Table 7.8: Confusion Matrix for Eye Detection using FREAK –PCA Descriptor.

	Eyes	***Non Eyes***
Eyes	83.42	16.58
Non Eyes	18.26	81.74

Table 7.9: Confusion Matrix for Eye Detection using FREAK -RP Descriptor.

	Eyes	***Non Eyes***
Eyes	83.22	16.78
Non Eyes	21.19	78.81

Table 7.10: Confusion Matrix for Eye Detection using FREAK – LPP Descriptor.

	Eyes	***Non Eyes***
Eyes	83.22	16.78
Non Eyes	18.67	81.33

Table 7.11: Confusion Matrix for Eye Detection using FREAK – SLPP Descriptor.

	Eyes	***Non Eyes***
Eyes	93.84	6.16
Non Eyes	12.67	87.33

Histogram of FREAK Descriptor

The Histogram of FREAK descriptor was found using the cell size as 4, block size as 2 and bin size as 20. Thus, the descriptor length was found to be 728 and this was reduced to 145 using different dimensionality reduction techniques. Tables 7.12-7.16 show the confusion matrices with this descriptor.

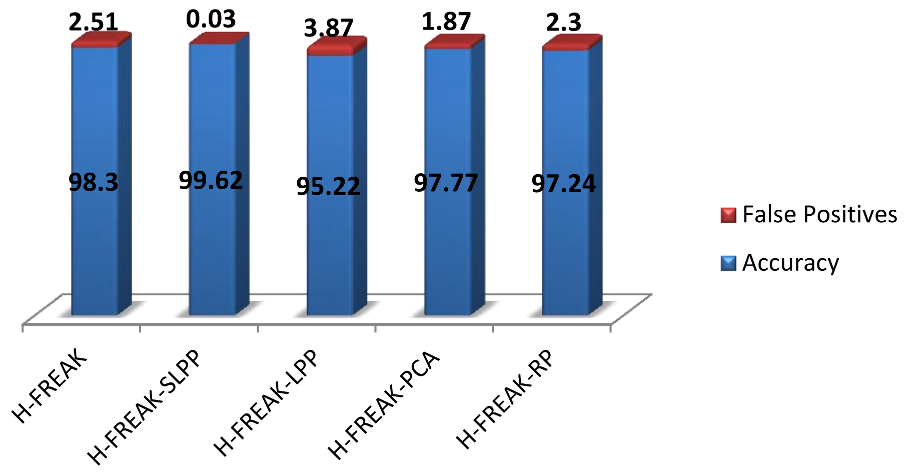

Figure 7.10: Accuracy and False Positives with Histogram of FREAK.

Table 7.12: Confusion Matrix for Eye Detection using Histogram of FREAK Descriptor.

	Eyes	***Non Eyes***
Eyes	98.30	1.7
Non Eyes	2.51	97.49

Table 7.13: Confusion Matrix for Eye Detection using Histogram of FREAK –PCA Descriptor.

	Eyes	***Non Eyes***
Eyes	97.77	2.23
Non Eyes	1.87	98.13

Table 7.14: Confusion Matrix for Eye Detection using Histogram of FREAK -RP Descriptor.

	Eyes	***Non Eyes***
Eyes	97.24	2.76
Non Eyes	2.3	97.70

Table 7.15: Confusion Matrix for Eye Detection using Histogram of FREAK – LPP Descriptor.

	Eyes	***Non Eyes***
Eyes	95.22	4.78
Non Eyes	3.87	96.13

Table 7.16: Confusion Matrix for Eye Detection using Histogram of FREAK – SLPP Descriptor.

	Eyes	***Non Eyes***
Eyes	99.62	0.38
Non Eyes	0.03	99.97

<u>LBP Descriptor</u>

The LBP descriptor was found using the 3x3 block with patch size 25x50. The descriptor length was found to be 1250 and was reduced to 625 using different dimensionality reduction techniques. Tables 7.17-7.21 show the confusion matrices with LBP descriptor.

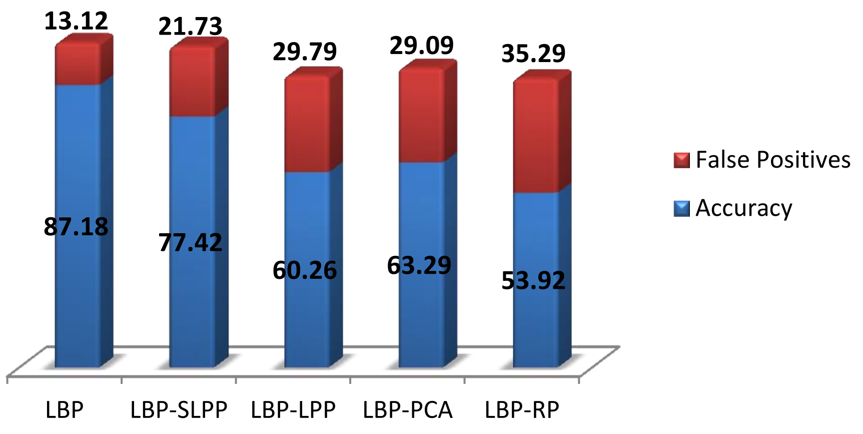

Figure 7.11: Accuracy and False Positives with LBP.

Table 7.17: Confusion Matrix for Eye Detection using LBP Descriptor.

	Eyes	***Non Eyes***
Eyes	87.18	12.82
Non Eyes	13.12	86.88

Table 7.18: Confusion Matrix for Eye Detection using LBP –PCA Descriptor.

	Eyes	***Non Eyes***
Eyes	63.29	36.71
Non Eyes	29.09	70.91

Table 7.19: Confusion Matrix for Eye Detection using LBP -RP Descriptor.

	Eyes	***Non Eyes***
Eyes	53.92	46.08
Non Eyes	35.29	64.71

Table 7.20: Confusion Matrix for Eye Detection using LBP – LPP Descriptor.

	Eyes	***Non Eyes***
Eyes	60.26	39.74
Non Eyes	29.79	70.21

Table 7.21: Confusion Matrix for Eye Detection using LBP – SLPP Descriptor.

	Eyes	***Non Eyes***
Eyes	77.42	22.18
Non Eyes	21.73	78.27

Histogram of LBP Descriptor

The Histogram of LBP descriptor was found using the cell size as 8, block size as 2 and bin size as 9. Thus, the descriptor length was found to be 648 and this was reduced to 130 using different dimensionality reduction techniques. Tables 7.22-7.26 show the confusion matrices with this descriptor.

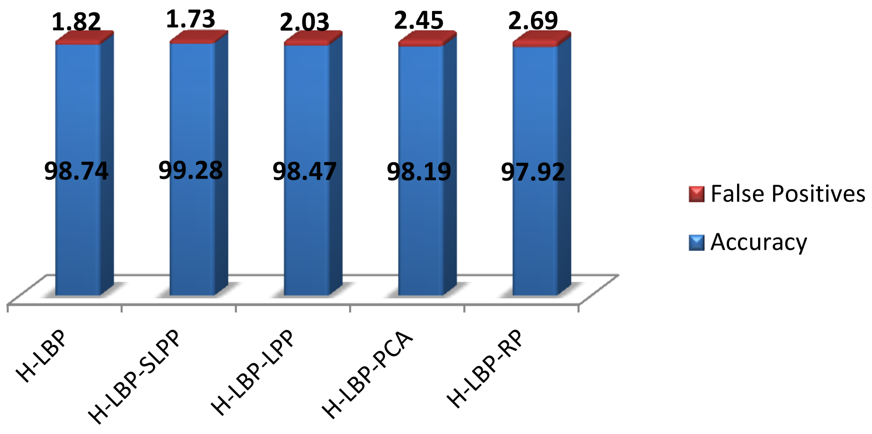

Figure 7.12: Accuracy and False Positives with Histogram of LBP.

Table 7.22: Confusion Matrix for Eye Detection using Histogram of LBP Descriptor.

	Eyes	***Non Eyes***
Eyes	98.74	1.26
Non Eyes	1.82	98.18

Table 7.23: Confusion Matrix for Eye Detection using Histogram of LBP –PCA Descriptor.

	Eyes	***Non Eyes***
Eyes	98.19	1.81
Non Eyes	2.45	97.55

Table 7.24: Confusion Matrix for Eye Detection using Histogram of LBP -RP Descriptor.

	Eyes	***Non Eyes***
Eyes	97.92	2.08
Non Eyes	2.69	97.31

Table 7.25: Confusion Matrix for Eye Detection using Histogram of LBP – LPP Descriptor.

	Eyes	***Non Eyes***
Eyes	98.47	1.53
Non Eyes	2.03	97.97

Table 7.26: Confusion Matrix for Eye Detection using Histogram of LBP – SLPP Descriptor.

	Eyes	***Non Eyes***
Eyes	99.28	0.72
Non Eyes	1.73	98.27

Our results demonstrate that eye detection using dimensionality reduction gave results which are comparable to that of the feature descriptor alone while the feature dimensionality is significantly reduced. The histogram based features are discriminative and efficient, which makes them good candidates for real time eye detection.

It was observed that with the use of supervised locality preserving projections (SLPP), false positives were reduced. With SLPP, the number of false positives were 0.91% for HOG, 0.03%

for histogram of FREAK, and 1.73% for histogram of LBP. Without using SLPP, the number of false positives were 1.52% for HOG, 2.51% for histogram of FREAK, and 1.82% for histogram of LBP.

To demonstrate the effectiveness of the eye detector on full images, we used a sliding window approach along with the SVM classification. The eye detection results for representative images from the BioID database and the FERET database, are shown in Figures 7.13 and 7.14 respectively. The results for BioID and FERET datasets are shown in Table 7.27 and 7.29 respectively.

Table 7.27: Eye Detection Results on BioID with HOG and different Dimensionality Reduction Techniques.

Method	***Percent Correct***		
	Left Eye	***Right Eye***	***Both Eyes***
HOG	97.14	96.32	96.25
HOG-SLPP	96.65	96.38	96.18
HOG-LPP	95.63	92.28	91.54
HOG-PCA	96.79	96.25	96.04
HOG-RP	96.32	96.05	95.63

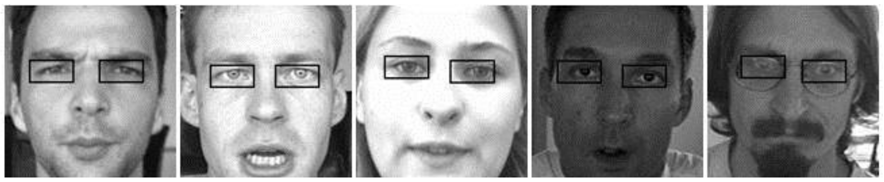
(a) HOG descriptor results

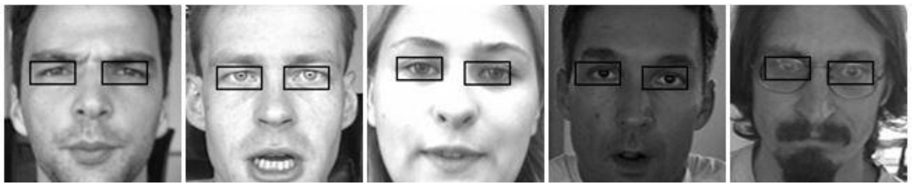
(b) HOG-SLPP descriptor results

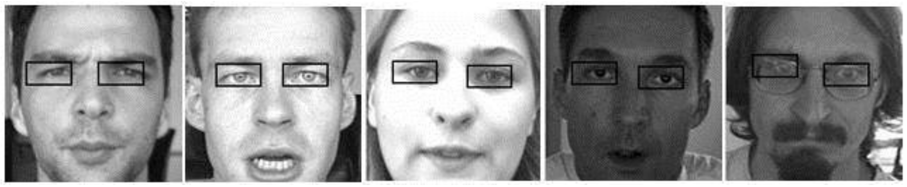
(c) HOG-LPP descriptor results

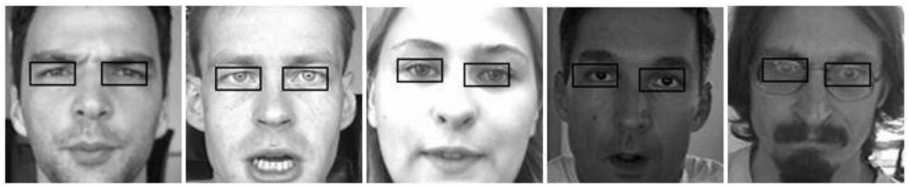
(d) HOG-PCA descriptor results

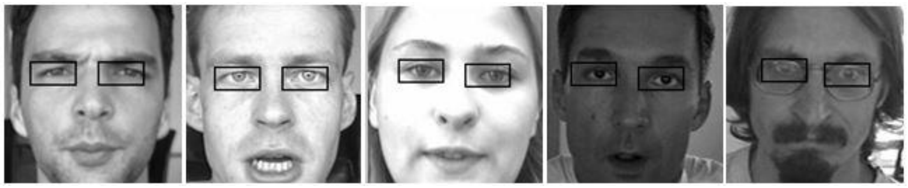
(e) HOG-RP descriptor results

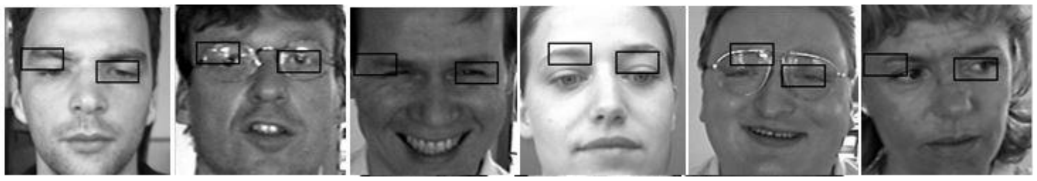
(f) Examples of false positives

Figure 7.13: Eye Detector examples in BioID database (a) HOG Descriptor, (b) HOG-SLPP Descriptor, (c) HOG-LPP Descriptor, (d) HOG-PCA Descriptor, (e) HOG-RP Descriptor, and (f) Examples of False Positives.

Table 7.28 shows a comparison of eye detection results on the BioID dataset using our approach and other state-of-the-art approaches. The method in [24] used Haar wavelet coefficients with SVM classifier and achieved an accuracy of 96.1% on the BioID dataset, while the method of [64] achieved an accuracy of 91.78% in locating eyes using SVM classifier. The approach in [23] uses isocentric patterns to locate the eye center and achieved an accuracy of 91.67%.

Table 7.28 Comparison of BioID Results using Different Approaches.

Authors	***Method***	***Accuracy***
Wang, Yang [64]	Clustering and binary template matching	91.78%
Campadelli, Lanzarotti, Lipori [24]	Support Vector Machine with Haar Wavelet coefficient	96.1%
Valenti, Gevers [23]	Isocentric Patterns	91.67%
Our Approach [44]	Support Vector Machine with HOG	96.25%

Table 7.29: Eye Detection Results on FERET with HOG and different Dimensionality Reduction Techniques.

Method	***Percent Correct***		
	Left Eye	***Right Eye***	***Both Eyes***
HOG	98.95	98.33	98.06
HOG-SLPP	99.11	98.99	98.59
HOG-LPP	98.76	97.7	97.62
HOG-PCA	98.68	97.89	97.45
HOG-RP	98.68	98.07	97.62

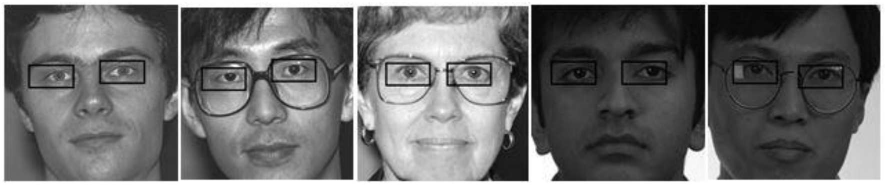

(a) HOG descriptor results

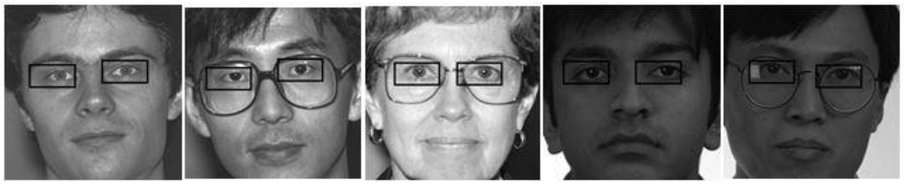

(b) HOG-SLPP descriptor results

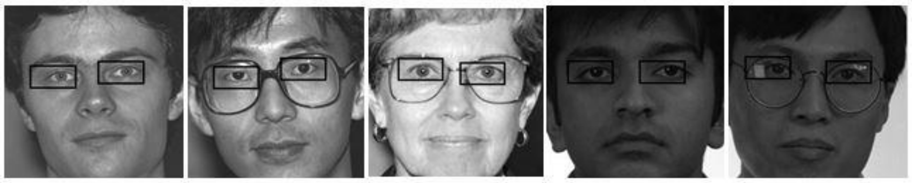

(c) HOG-LPP descriptor results

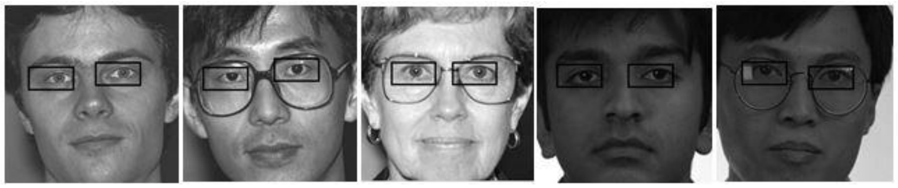

(d) HOG-PCA descriptor results

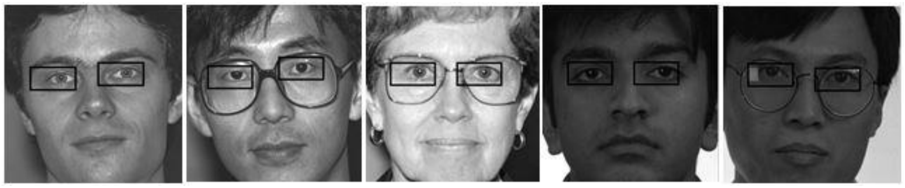

(e) HOG-RP descriptor results

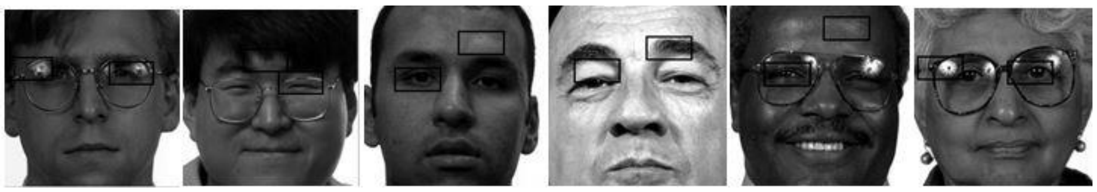

(f) Examples of false positives

Figure 7.14: Eye Detector examples in FERET database (a) HOG Descriptor, (b) HOG-SLPP Descriptor, (c) HOG-LPP Descriptor, (d) HOG-PCA Descriptor, (e) HOG-RP Descriptor, and (f) Examples of False Positives.

Table 7.30 shows a comparison of eye detection results on the FERET dataset using our approach and other state-of-art approaches. The method in [24] used Haar wavelet coefficients with SVM classifier and achieved an accuracy of 96.4% on the FERET dataset, while the method of [65] achieved an accuracy of 98.3% in locating eyes using SVM classifier. The approach in [23] uses isocentric patterns to locate the eye center and achieved an accuracy of 96.27%.

Table 7.30: Comparison of FERET Results using Different Approaches.

Authors	***Method***	***Accuracy***
Monzo, Albiol, Sastre [65]	Adaboost + Haar, SVM + HOG	98.3%
Campadelli, Lanzarotti, Lipori [24]	Support Vector Machine with Haar Wavelet coefficient	96.4%
Valenti, Gevers [23]	Isocentric Patterns	96.27%
Our Approach [44]	Support Vector Machine with HOG+SLPP	98.59%

The eye detection results in the BioID and FERET database demonstrate that the HOG, HOG-SLPP, HOG-PCA and HOG-RP descriptors perform well and their accuracy results are comparable within one percent. The overall performance of detector is a bit lower than the detector performance using 10-fold cross validation for patch classification due to wider variability in the appearance of patches in full images.

7.3 CalTech-101 Testing

The CalTech-101 dataset consists of 102 object categories and each category consists of 31 to 800 images per category. These are colored images with size around 200 x 300 pixels and were converted to gray scale and normalized to size 50 x 75. Table 7.31 shows accuracy results with

10-fold cross validation with 30 samples per category with HOG descriptor. Table 7.32 shows accuracy with 30 samples for training and 50 for testing with HOG-SLPP descriptor.

Table 7.31: Results with CalTech-101, 10-Fold Cross Validation, 30 Samples per Category.

SLPP	***LPP***	***PCA***	***RP***
78.3 %	63.4 %	67 %	58 %

Table 7.32: Results with CalTech-101, 30 Training Samples and 50 Testing Samples.

Method	***SLPP***
Overlap	91 %
No-overlap	64 %

Table 7.33: Comparison of Classification Results of CalTech-101 with Different Approaches.

Authors	***Method***	***Training***		***Accuracy***
Zeiler, Fergus [63]	Convolutional Networks	Train – 30 Test – 50		86.5%
Yang, Li, Tian, Duan, Gao [62]	Multiple Kernel Learning with SIFT and PHOG	Train – 30 Test - 15		84.3%
Bos, Zisserman, Munoz [66]	Random forests and ferns with PHOG for image classification	Train – 30 Test - 50		81.3%
Our Approach	Support Vector Machine with HOG+SLPP	Train – 30 Test - 50	Overlap	91%
			No-overlap	64%
		10-fold CV	All Data	96%
			30 samples	78.3%

Table 7.33 shows a comparison of classification results on Caltech-101 dataset using our approach and other state-of-art approaches. The method in [63] uses convolutional networks for

classification and achieved an accuracy of 86.5% on the Caltech-101, while the method of [62] achieved an accuracy of 84.3% using group sensitive multiple kernel learning approach which accommodates intra-class diversity and inter-class correlation for object recognition. The approach in [66] uses random forest and ferns with PHOG for image classification and achieved an accuracy of 81.3%.

7.4 Image Descriptors

In this section, the performance of different image feature descriptors is evaluated and compared. The evaluation was done using 10-fold cross validation technique on the eye database created from BioID and FERET database and Caltech-101.

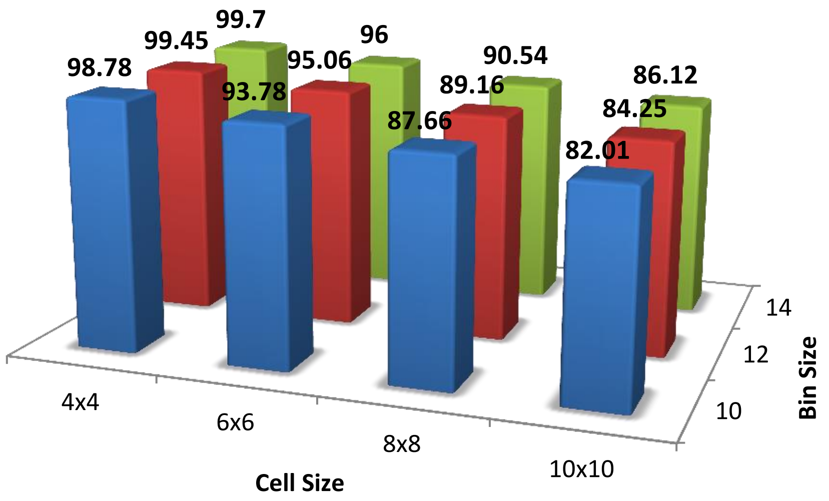

Figure 7.15: Accuracy for CalTech-101 as Cell Size and Bin Size was varied for HOG-SLPP.

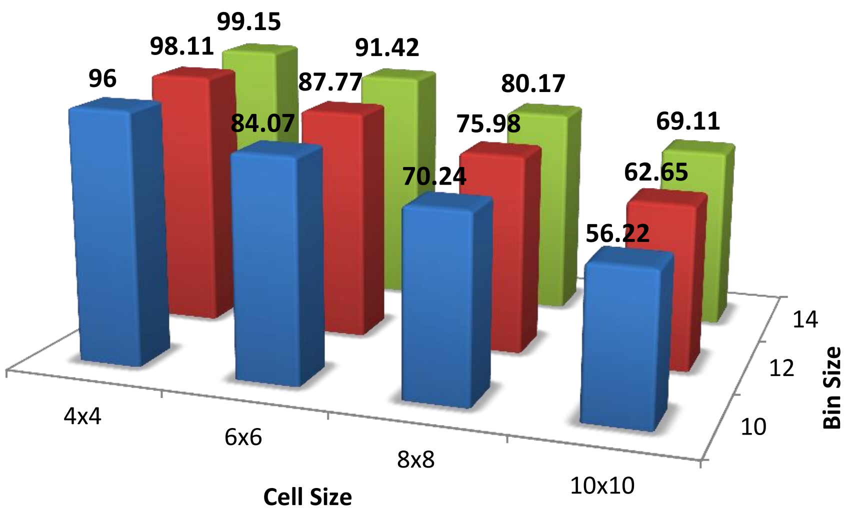

Figure 7.16: Accuracy for CalTech-101 as Cell Size and Bin Size was varied for H-FREAK – SLPP.

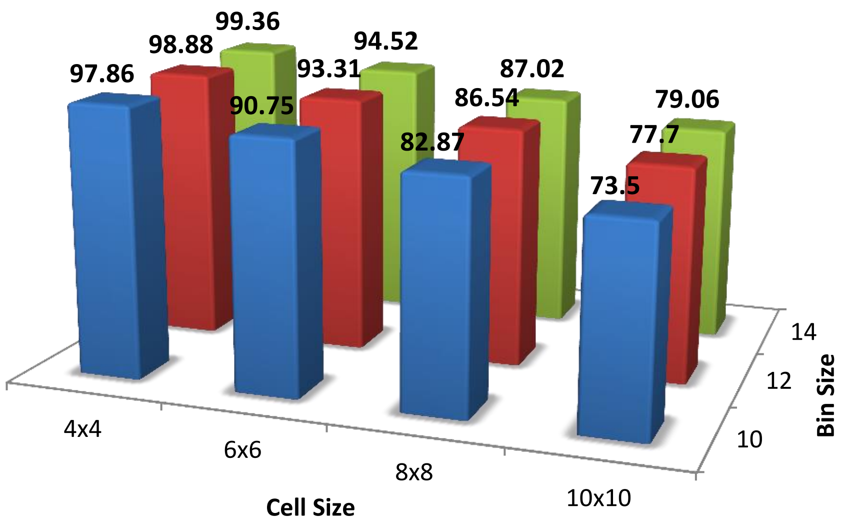

Figure 7.17: Accuracy for CalTech-101 as Cell Size and Bin Size was varied for H-LBP – SLPP.

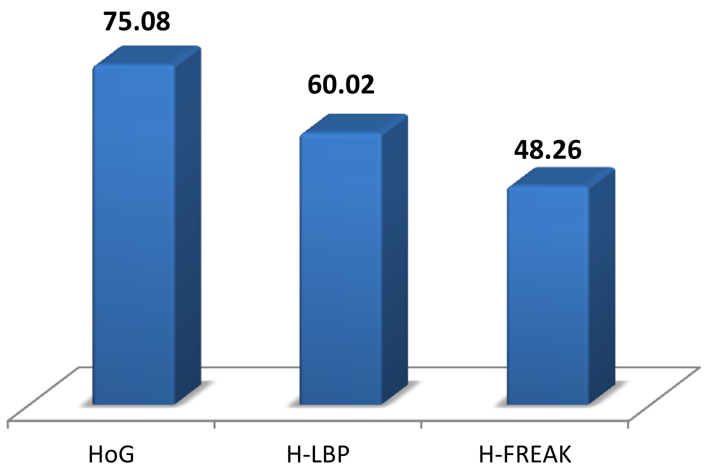

Figure 7.18: Accuracy for CalTech-101 with different Descriptors.

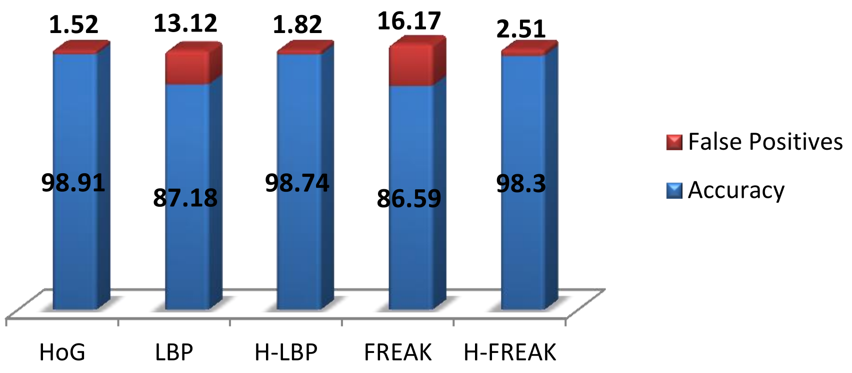

Figure 7.19: Eye Detection Results.

It was found from the experiments that Histogram of Oriented Gradients feature descriptor outperforms the binary feature descriptors. An accuracy of 98.91% was achieved with the eye database and accuracy of 75.08% was achieved with CalTech-101 dataset. In addition, it was observed that histogram of binary descriptors outperformed binary descriptors for object detection. Accuracy of 87.18% and 86.59% was achieved with Local Binary pattern and FREAK descriptor respectively whereas this was increased to 98.74% and 98.3% when histogram of LBP and Histogram of FREAK was used as a feature descriptor respectively. This was because support vector machines use Euclidean distance as the distance measure.

7.5 Dimensionality Reduction

In this section, performance of different dimensionality reduction methodologies is evaluated and compared. The evaluation was done using 10-fold cross validation technique on Caltech-101. The object images were cropped using the given annotations and were resized to 50 x 75. The classification performance was tested using 10-fold cross validation technique. Histogram of descriptors was found using cell size 6, block size 2 and bin size 14. The results with different descriptors are as shown in Table 7.34.

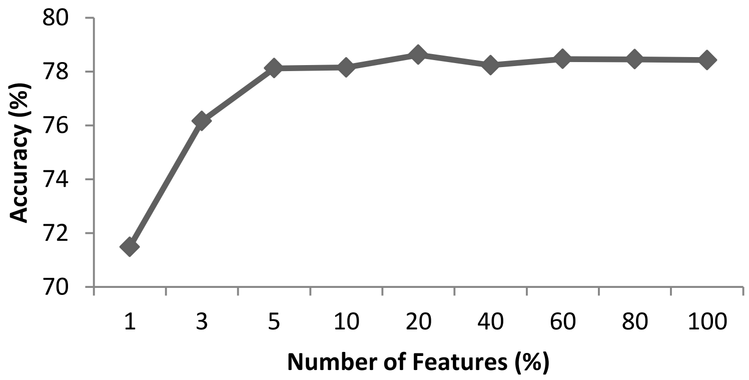

Figure 7.20: Graph showing Accuracy as we increase the Number of Components CalTech-101.

It was found by experiments that the dimensions of the data can be reduced to 5% using different dimensionality reduction techniques.

Table 7.34: Results with CalTech-101.

Descriptor	***Original***	***S-LPP***	***LPP***	***PCA***	***RP***
HOG	75.08	96	75.93	78.12	78.15
H-LBP	60.2	94.52	43.59	62.38	47.76
H-FREAK	48.26	91.42	51.25	49.8	45.27

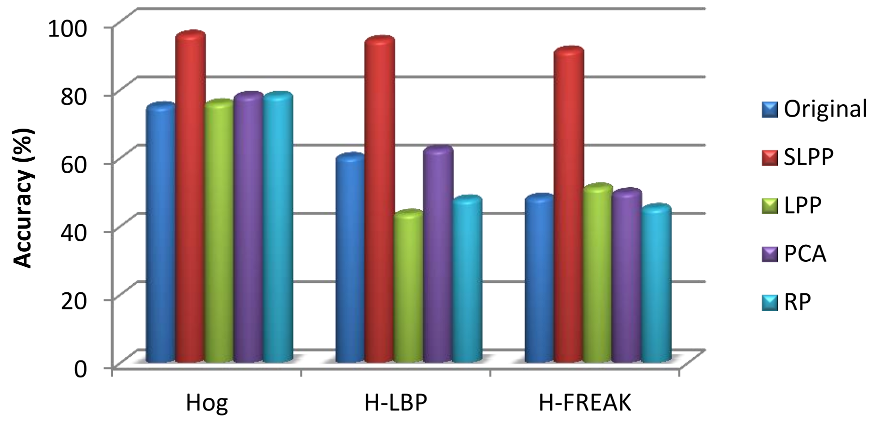

Figure 7.21: Results with different Descriptors and Dimensionality Reduction techniques for CalTech-101.

Experimental results showed that using dimensionality reduction increases the performance of classification. It was observed that dimensionality reduction with histogram of oriented gradients gave better accuracy as compared to histogram of oriented gradients alone. Increase of 20.9%, 0.85%, 0.04%, and 0.07% was observed with supervised Locality preserving projection, unsupervised locality preserving projections, principal component analysis and random projections respectively.

It was found that supervised locality preserving projections worked best as compared to other dimensionality reduction techniques. With SLPP the classification accuracy was increased by 20.9%, 34.32% and 43.16% with histogram of oriented gradients, histogram of LBP and histogram of FREAK feature descriptor respectively for Caltech-101. Additionally, it was observed that Random Projections was fast to compute and gave comparable results as principal component analysis and unsupervised locality preserving projections.

Chapter 8

Conclusions

This thesis explores object detection using different dimensionality reduction techniques on HOG or binary image descriptors. The major contributions of this thesis include an efficient eye detection approach using dimensionality reduction on histogram of oriented gradients as a feature descriptor. Also, histogram based FREAK descriptor was proposed as a feature descriptor for successful object detection. Furthermore, different feature descriptors and different dimensionality reduction techniques were analyzed and evaluated for object detection.

Histogram based feature descriptors such as Histogram of Oriented Gradients (HOG), histogram of FREAK (H-FREAK) and histogram of Local Binary Pattern (H-LBP) were explored as good features for object detection. It was found that Histogram of Oriented gradients worked best both in accuracy and speed as compared to binary descriptors. Accuracy of 75% was obtained by using Histogram of Oriented Gradients as a feature descriptor for CalTech-101 dataset whereas Histogram of FREAK and Histogram of LBP descriptor gave an accuracy of 48.26 % and 60.2% respectively. In case of eye detection, accuracy of 98.91% was achieved with HOG and accuracy of 98.3% and 98.7% was achieved with H-FREAK and H-LBP feature descriptor respectively.

Also, since histogram based descriptors can be of large dimensions, different dimensionality reduction techniques were explored in order to reduce the dimensions of the image descriptors. Experimental results showed that supervised locality preserving projections worked best as compared to other dimensionality reduction techniques. With SLPP the classification accuracy was increased by 43.16% with H-FREAK feature descriptor for Caltech-101. Furthermore, it was observed that Random Projections was fast to compute and gave comparable results as principal component analysis.

The future challenges to this work involve using binary descriptors with Hamming distance as the distance measure in support vector machines and compare these results for object detection with Euclidean distance as the distance measure in support vector machines. Another challenge in the improvement of the object detection system would be to use deformable parts model with Histogram based descriptors and supervised locality preserving projection as the dimensionality reduction technique.

References

[1] T. Malisiewicz, A. Gupta and A. Efros, "Ensemble of Exemplar-SVMs for Object Detection and Beyond," in *International Conference on Computer Vision*, Spain, 2011.

[2] P. Deniz, G. Bueno, J. Salido and F. Torre, "Face Recognition using Histogram of Oriented Gradients," *Pattern Recognition Letters*, vol. 32, no. 12, pp. 1598-1603, 2011.

[3] J. M. Keller, M. R. Gray and J. A. Givens, "A fuzzy k-nearest neighbor algorithm," *IEEE Transactions on Systems, Man and Cybernetics*, vol. 4, pp. 580-585, 1985.

[4] M. Mitchell, J. Dodge, A. Goyal, K. Yamaguchi, K. Stratos, X. Han, A. Mensch, A. Berg, T. Berg and H. Daume, "Midge: Generating Image Descriptors from Computer Vision Detections," in *European Chapter of the Association for Computational Linguistics*, France, 2012.

[5] N. Dalal and B. Triggs, "Histogram of Oriented Gradients for Human Detection," in *IEEE Computer Vision and Pattern Recognition*, California, 2005.

[6] Y. Rodriguez and S. Marcel, "Face Authentication using Adapted Local Binary Pattern Histograms," in *European Conference on Computer Vision*, Graz, Austria, 2006.

[7] J. Gall, A. Yao, N. Razavi and V. Gool, "Hough Forests for Object detection, tracking and action recognition," in *IEEE Transaction on Pattern Analysis and Machine Intelligence*, 2011.

[8] J. Gall and V. Lempitsky, "Class-specific hough forests for object detection," in *Decision Forests for Computer Vision and Medical Image Analysis*, London, 2013.

[9] D. Tran and D. Forsyth, "Configuration Estimates Improve Pedestrian Finding," in *Neural Information Processing Systems*, Vancouver, 2007.

[10] S. Leutenegger, C. Margarita and R. Y. Siegwart, "Brisk: Binary Robust Invariant Scalable Keypoints," in *IEEE International Conference on Computer Vision*, Spain, 2011.

[11] R. O. Duda, P. E. Hart and D. G. Stork, Pattern Classification, Wiley, 2000.

[12] A. Ghodsi, "Dimensionality Reduction: A Short Tutorial," Department of Actuarial Science, University of Waterloo, Ontario, Canada, 2006.

[13] E. Bingham and H. Mannila, "Random Projection in Dimensionality Reduction: Application to Image and Text Data," in *ACM International Conference on Knowledge Discovery and Data Minning*, San Francisco, CA, 2001.

[14] D. Achlioptas, "Database-friendly Random Projections: Johnson-Lindenstrauss with Binary Coins," *Journal of Computer and System Sciences*, vol. 4, no. 66, pp. 671-687, 2003.

[15] X. He and P. Niyogi, "Locality Preserving Projections," *Neural Information Processing Systems*, vol. 16, pp. 234-241, 2003.

[16] M. Uricar, V. Franc and V. Hlavac, "Detector of Facial Landmarks Learned by the Structured Output SVM," in *International Conference on Computer Vision Theory and Applications (VISAPP)*, Rome, 2012.

[17] J. Shermina, "Application of Locality Preserving Peojections in Face Recognition," *International Journal of Advanced Computer Science and Applications*, vol. 1, no. 3, 2010.

[18] C. Papageorgiou and T. Poggio, "A Trainable System for Object Detection," *International Journal of Computer Vision*, vol. 38, no. 1, pp. 15-30, 2000.

[19] . A. Rowley, S. Baluja and T. Kanade, "Neural Network based Face Detection," *IEEE Transaction on Pattern Analysis and Machine Intelligence,* vol. 20, no. 1, pp. 29-38, 1998.

[20] E. Miluzzo, T. Wang and A. T. Campbell, "EyePhone: Activating Mobile Phones with your Eyes," in *ACM SIGCOMM Workshop on Networking Systems, and Applications on Mobile Handhelds*, New Delhi, 2010.

[21] Z. Zhu and Q. Ji, "Robust Real-Time Eye Detection and Tracking under variable Lighting Conditions and various Face Orientations," *Computer Vision and Image Understanding,* vol. 98, no. 1, pp. 124-154, 2005.

[22] T. F. Cootes and C. J. Taylor, "Active Shape Models Search using Local Grey-Level Models: A Quantitative Evaluation," *British Machine Vision Conference,* vol. 93, pp. 639-648, 1993.

[23] R. Valenti and T. Gevers, "Accurate Eye Center Location through Invariant Isocentric Patterns," *IEEE Transaction on Pattern Analysis and Machine Intelligence,* vol. 34, no. 9, pp. 1785-1798, 2012.

[24] P. Campadelli, R. Lanzarotti and G. Lipori, "Precise Eye Localization through a General-to-Specific Model Definition," *British Machine Vision Conference,* pp. 187-196, 2006.

[25] O. Regniers, J. Costa, G. Grenier and L. Bombrun, "Texture based Image Retrieval and Classification of Very High Resolution Maritime Pine Forest Images," in *IEEE International Geoscience and Remote Sensing Symposium*, Melbourne, 2013.

[26] T. Barbu, "SVM-based Human Cell Detection technique using Histogram of Oriented Gradients," in *WEAS International Conference on Mathematical Methods for Information Sciences and Economics*, 2012.

[27] X. Cao, C. Wu, P. Yan and X. Li, "Linear SVM Classification using Boosting HOG Features for Vehicle Detection in Low Altitude Airborne Videos," in *IEEE International Conference on Image Processing*, Orlando, 2011.

[28] M. Calonder, V. Lepetit, C. Strecha and P. Fua, "BRIEF: Binary Robust Independent Elementary Features," in *European Conference on Computer Vision*, Berlin, 2010.

[29] J. Zhang, K. Huang, Y. Yu and T. Tan, "Boosted Local Structured HOG-LBP for Object Localization," in *IEEE Conference on Computer Vision and Pattern Recognition*, Rhode Island, 2011.

[30] X. Wang, T. X. Han and S. Yan, "An HOG-LBP Human Detector with Partial Occlusion Handling," in *IEEE International Conference on Computer Vision*, Kyoto, Japan, 2009.

[31] T. Ahonen, A. Haddid and M. Pietikainen, "Face Description with Local Binary Patterns: Application to Face Recognition," *IEEE Transaction on Pattern Analysis and Machine Intelligence,* vol. 28, no. 12, pp. 2037-2041, 2006.

[32] T. Ojala and M. Pietikainen, "Multiresolution Gray-Scale and Rotation Invariant Texture Classification with Local Binary Patterns," *IEEE Transaction on Pattern Analysis and Machine Intelligence,* vol. 24, no. 7, pp. 971-987, 2002.

[33] L. Szasz-Toth, "Combination of Classifier Cascades and Training Sample Selection for Robust Face Detection," in *Universitat Karlsruhe*, Germany, 2009.

[34] A. Bosch, A. Zisserman and X. Munoz, "Representing Shape with a Spatial Pyramid Kernel," in *ACM International Conference on Image and Video Retrieval*, Amsterdam, 2007.

[35] M. Marszalek, C. Schmid, H. Harzallah and J. Weijer, "Learning Object Representations for Visual Object Class Recognition," in *Visual Recognition Challenge Workshop, in conjunction with ICCV*, Brazil, 2007.

[36] D. G. Lowe, "Distinctive Image Features from Scale-Invariant Keypoints," *International Journal of Computer Vision*, vol. 60, no. 2, pp. 91-110, 2004.

[37] Y. Ke and R. Sukthankar, "PCA-SIFT: A more distinctive representation for Local Image Descriptors," in *IEEE Computer Society Conference on Computer Vision and Pattern Recognition*, Washington DC, 2004.

[38] J. Lin and D. Gunopulos, "Dimensionality Reduction by Random Projection and Latent Semantic Indexing," in *SIAM International Conference on Data Mining*, San Francisco, 2003.

[39] A. Alahi, R. Ortiz and P. Vandergheynst, "FREAK: Fast Retina Keypoint," in *IEEE Conference on Computer Vision and Pattern Recognition*, Rhode Island, 2012.

[40] A. Vedaldi, V. Gulshan, M. Varma and A. Zisserman, "Multiple Kernel for Object Detection," in *IEEE International Conference on Computer Vision*, Kyoto, Japan, 2009.

[41] W. R. Schwartz, A. Kembhavi, D. Hardwood and L. S. Davis, "Human Detection using Partial Least Square Analysis," in *IEEE International Conference on Computer Vision*, Kyoto, Japan, 2009.

[42] M. Pietikainen, A. Hadid, G. Zhao and T. Ahonen, "Local Binary Patterns for Still Images," *Computer Vision using Local Binary Patterns*, vol. 40, pp. 13-47, 2011.

[43] B. E. Boser, I. M. Guyon and V. N. Vapnik, "A Training Algorithm for Optimal Margin Classifiers," in *Proceedings of the Conference on Learning Theory*, 1992.

[44] A. Savakis, R. Sharma and M. Kumar, "Efficient Eye Detection using HOG-PCA Descriptor," in *IS&T/SPIE Electronic Imaging Conference, Imaging and Multimedia Analytics in a Web and Mobile World* , San Francisco, 2014.

[45] S. Agarwal and A. Awan, "Learning to Detect Objects in Images via a Sparse, Part Based Representation," *IEEE Transaction on Pattern Analysis and Machine Intelligence,* vol. 26, no. 11, pp. 1475-1490, 2004.

[46] X. R. Chen and A. Yuille, "Detecting and Reading Text in Natural Scenes," in *IEEE International Conference on Computer Vision and Pattern Recognition*, Washington DC, 2004.

[47] E. Osuna, R. Freund and F. Girosi, "Training Support Vector Machines: An Application to Face Detection," in *IEEE Conference on Computer Vision and Pattern Recognition*, Puerto Rico, 1997.

[48] C. P. Papageorgiou and T. Poggio, "A Trainable Object Detection System: Car Detection in Static Images," *MIT AI Memo,* no. 180, 1999.

[49] P. F. Felzenszwalb, D. A. McAllester and D. Ramanan, "A Discriminatively Trained, Multiscale, Deformable Part Model," in *IEEE International Conference on Computer Vision and Pattern Recognition*, Alaska, 2008.

[50] P. J. Philips, H. Wechsler, J. Huang and P. J. Rauss, "The FERET database and Evaluation procedure for Face Recognition Algorithms," *Image and Vision Computing Journal,* vol. 16, no. 5, pp. 296-306, 1998.

[51] P. J. Philips, H. Moon, S. A. Rizvi and P. J. Rauss, "The FERET Evaluation Methodology for Face Recognition Algorithms," *IEEE Transaction on Pattern Analysis and Machine Intelligence,* vol. 22, pp. 1090-1104, 2000.

[52] D. Comaniciu and P. Meer, "Robust Analysis of Feature Spaces: Color Image Segmentation," *IEEE Transaction on Pattern Analysis and Machine Intelligence,* vol. 24, pp. 603-619, 2002.

[53] L. Fei-Fei, R. Fergus and P. Perona, "One-Shot Learning of Object Categories," *IEEE Transaction on Pattern Analysis and Machine Intelligence,* vol. 28, no. 4, pp. 594-611, 2006.

[54] C. Garcia and M. Delakis, "Convolutional Face Finder: A Neural Architecture for Fast and Robust Face Detection," *IEEE Transaction on Pattern Analysis and Machine Intelligence,* vol. 26, no. 11, pp. 1408-1423, 2004.

[55] M. Brown and D. G. Lowe, "Automatic Panoramic Image Stitching using Invariant Features," *International Journal of Computer Vision,* vol. 74, no. 1, pp. 59-73, 2007.

[56] T. Vetter, M. J. Jones and T. Poggio, "A Bootstrapping Algorithm for Learning Linear Models of Object Classes," in *IEEE Conference on Computer Vision and Pattern Recognition,* Puerto Rico, 1997.

[57] P. Viola and M. J. Jones, "Robust Real-Time Face Detection," *International Journal of Computer Vision,* vol. 57, no. 2, pp. 137-154, 2004.

[58] C. C. Chang and C. J. Lin, "LIBSVM: A Library for Support Vector Machines," *ACM Transactions on Intelligent Systems and Technology,* vol. 2, no. 3, 2011.

[59] P. S. Hiremath and J. Pujari, "Content Based Image Retrieval using Color, Texture and Shape Features," in *IEEE International Conference on Advanced Computing and Communications,* Guwahati, India, 2007.

[60] A. Saxena, A. Gupta and A. Mukerjee, "Non-Linear Dimensionality Reduction by Locally Linear Isomaps," in *Neural Information Processing Systems,* Berlin, 2004.

[61] M. Belkin and P. Niyogi, "Laplacian Eigenmaps for Dimensionality Reduction and Data Representation," *Neural Computation,* vol. 15, no. 6, pp. 1372-1396, 2003.

[62] J. Yang, Y. Li, Y. Tian, L. Duan and W. Gao, "Group-Sensitive Multiple Kernel Learning for Object Categorization," in *IEEE International Conference on Computer Vision*, Kyoto, Japan, 2009.

[63] M. D. Zeiler and R. Fergus, "Visualizing and Understanding Convolutional Networks," in *ARXIV*, 2013.

[64] Q. Wang and J. Yang, "Eye Detection in Facial Images with Unconstrained Background," *Journal of Pattern Recognition Research*, vol. 22, no. 3, pp. 471-480, 2011.

[65] D. Monzo, A. Albiol and J. Sastre, "Precise Eye Localization using HOG Descriptors," *Machine Vision and Applications*, vol. 22, no. 3, pp. 471-480, 2011.

[66] A. Bosch, A. Zisserman and Z. Munoz, "Image Classification using Random Forests and Ferns," in *IEEE International Conference on Computer Vision*, Brazil, 2007.

[67] P. Scovanner, S. Ali and S. M. Shah, "A 3-Dimensional SIFT Descriptor and its Application to Action Recognition," in *ACM International Conference on Multimedia*, Germany, 2007.

[68] J. Sivic, B. C. Russell, A. A. Efros, A. Zisserman and W. T. Freeman, "Discovering Objects and their Location in Images," in *IEEE International Conference on Computer Vision*, Beijing, 2005.